

**Synthesis and Characterization of Cobalt/Manganese Bimetallic  
Nanocatalyst Prepared via Reverse Microemulsion Method**

by

Mohamad Suffian Bin A. Rahman (12659)

Dissertation submitted in partial fulfillment of  
the requirements for the  
Bachelor of Engineering (Hons)  
(Chemical Engineering)

Supervisor: Dr. Rashidah Binti Mohd Pilus  
Co-Supervisor: Dr. Noor Asmawati Binti Mohd Zabidi

AUGUST 2013

Universiti Teknologi PETRONAS  
Bandar Seri Iskandar  
31750 Tronoh  
Perak Darul Ridzuan

CERTIFICATION OF APPROVAL

**Synthesis and Characterization of Cobalt/Manganese Bimetallic  
Nanocatalyst Prepared via Reverse Microemulsion Method**

by

Mohamad Suffian Bin A. Rahman (12659)

A project dissertation submitted to  
Chemical Engineering Program  
Universiti Teknologi PETRONAS  
in partial fulfillment of the requirements for the  
Bachelor of Engineering (Hons)  
(Chemical Engineering)

Approved by:

---

Dr. Rashidah Binti Mohd Pilus

UNIVERSITI TEKNOLOGI PETRONAS  
TRONOH, PERAK  
AUGUST 2013

## CERTIFICATION OF ORIGINALITY

This is to certify that I am responsible for the work submitted in this project, that the original work is my own except as specified in the references and acknowledgements, and that the original work contained herein have not been undertaken or done by unspecified sources or persons.

---

MOHAMAD SUFFIAN BIN A. RAHMAN

## ABSTRACT

The bimetallic cobalt-manganese nanocatalyst was synthesized via reverse microemulsion method. The reverse microemulsion was used as an alternative route to prepare the nanocatalyst rather than common catalyst preparation route, impregnation method as the later have reported problem with the metal dispersion. In this project, the main objective is to synthesize well-dispersed bimetallic nanocatalyst consisting of cobalt-manganese in different composition on silica support via reverse microemulsion method, to study the properties of catalyst by applying several characterization methods and to study the catalytic performance in a Fischer-Tropsch (FT) reaction. The following compositions were prepared which are pure cobalt, pure manganese, 95Co5Mn/SiO<sub>2</sub>, 88Co12Mn/SiO<sub>2</sub> and 76Co24Mn/SiO<sub>2</sub>. The nanocatalyst was analyzed by using Transmission Electron Microscopy (TEM), Field Emission Scanning Electron Microscopy (FESEM) and Temperature Programmed Reduction (TPR). The performance of the nanocatalyst for FT reaction was studied in a stainless steel fixed bed micro reactor. The average particle size of the nanocatalyst was 2-5 nm. TEM image show nanocatalyst 88Co12Mn/SiO<sub>2</sub> was better dispersed compared to other formulations. The TPR result of the 100Co/SiO<sub>2</sub> and 95Co5Mn/SiO<sub>2</sub> showed that these nanocatalysts were reduced at the temperatures of 690 °C and 645 °C, respectively. The reducibility was improved when 12 wt% Mn was added to Co-based nanocatalyst for 88Co12Mn/SiO<sub>2</sub> since the high temperature peak was shifted to lower temperature (536 °C). However, further increase in Mn content (24 wt%) had shifted the high temperature peak to higher temperature (600 °C). This indicates that the optimum Mn content (12 wt%) enhanced the reducibility of the Co-based nanocatalyst. The catalytic activity in the FT reaction varied with the content of Mn in the Co-based nanocatalyst. In conclusion, the highest CO conversion (20.5%) and C<sub>5+</sub> selectivity (12.6%) were obtained using 88Co12Mn/SiO<sub>2</sub> nanocatalyst.

## **ACKNOWLEDGEMENT**

First and foremost, thanks to God for His blessing and mercy in completing this final year project within 8 month. It would befit to extend my outstretched gratitude to my supervisor Dr. Rashidah binti Mohd Pilus, Fundamental and Applied Sciences Department, my co-supervisor Dr Noor Asmawati binti Mohd Zabidi and Dr. Sardar Ali, Centralized Analytical Laboratory, Universiti Teknologi PETRONAS. It is a privilege to be under her and his supervision. Even with their tight schedules as senior lecturer and high commitment to Universiti Teknologi PETRONAS, there was no moment where she and he fail to provide support and guidance. Her and his advices and moral support gave a sense of strength and confidence in conducting the final year project. Thousand appreciations to Dr. Rashidah binti Mohd Pilus's research grant, STIRF 28/2012 and Dr. Noor Asmawati binti Mohd Zabidi's research grant, FRGS (FRGS/1/2012/SG01/UTP/02/01) for funding my final year project.

Many thanks to the Final Year Project Coordinators and others involved for their unlimited contributions and efforts in providing students the guidelines and seminars in order to enlighten hopes of confidence. Not forget to thank all lab executive and technicians as their willingness to provide the facilities and entertain our demand during conducting the project.

Last but not least, thanks to all the Universiti Teknologi PETRONAS involved lecturers and students who have been contributing great efforts and ideas making this final year project a success.

## TABLE OF CONTENT

### CHAPTER 1: INTRODUCTION

|     |                                  |   |
|-----|----------------------------------|---|
| 1.1 | Background Study .....           | 1 |
| 1.2 | Problem Statement .....          | 2 |
| 1.3 | Objective of the Project.....    | 2 |
| 1.4 | Scope of Study .....             | 3 |
| 1.5 | Relevancy of the Project .....   | 3 |
| 1.6 | Feasibility of the Project ..... | 4 |

### CHAPTER 2: LITERATURE REVIEW

|     |   |   |
|-----|---|---|
| 2.1 | Introduction to Fischer-Tropsch Tehnology ..... | 5 |
| 2.2 | Fischer-Tropsch Product Distribution.....       | 6 |
| 2.3 | Catalyst for Fischer-Tropsch Synthesis.....     | 7 |
| 2.4 | Reverse Microemulsion Method .....              | 8 |

### CHAPTER 3: METHODOLOGY

|     |  |    |
|-----|--|----|
| 3.1 | Project Activities .....                     | 12 |
| 3.2 | Equipments and Chemicals .....               | 12 |
| 3.3 | Preparation of Co/Mn Nanocatalyst.....       | 14 |
| 3.4 | Characterization Method of Nanocatalyst..... | 16 |
| 3.5 | Microreactor Study.....                      | 17 |
| 3.6 | Project Flow .....                           | 21 |
| 3.7 | Key Milestones/Gantt's Chart.....            | 21 |

### CHAPTER 4: RESULT AND DISCUSSION

|       |   |    |
|-------|---|----|
| 4.1   | Catalyst Formulation .....                                | 22 |
| 4.2   | Characterization of Nanocatalyst.....                     | 22 |
| 4.2.1 | Morphology.....   | 22 |
| 4.2.2 | Field Emission Scanning Electron Microscopy (FESEM) ..... | 29 |
| 4.2.3 | Temperature Programmed Reduction (TPR) .....              | 29 |
| 4.2.4 | Fischer-Tropsch Performance .....                         | 31 |

### CHAPTER 5: CONCLUSION..... 35

|                  |    |
|------------------|----|
| REFERENCES ..... | 37 |
|------------------|----|

|               |    |
|---------------|----|
| APPENDIX..... | 39 |
|---------------|----|

## LIST OF FIGURES

|           |  |    |
|-----------|--|----|
| FIGURE 1  | Nanoparticles preparation using microemulsion technique .....            | 10 |
| FIGURE 2  | The schematic diagram of research project activities .....               | 12 |
| FIGURE 3  | Synthesis Setup .....  | 15 |
| FIGURE 4  | Synthesis Setup Schematic Drawing.....                                   | 15 |
| FIGURE 5  | Syringe .....  | 15 |
| FIGURE 6  | Microreactor Assembling.....   | 18 |
| FIGURE 7  | Catalyst Load Steps.....   | 19 |
| FIGURE 8  | MICROACTIVITY-References connected to GC.....                            | 20 |
| FIGURE 9  | Project Flow for the Research Project.....                               | 21 |
| FIGURE 10 | TEM images of S1 at different location .....                             | 22 |
| FIGURE 11 | TEM images of S2 at different location.....                              | 23 |
| FIGURE 12 | TEM images of S2 at different location.....                              | 23 |
| FIGURE 13 | TEM images of S4 at different location.....                              | 24 |
| FIGURE 14 | TEM images of S5 at different location.....                              | 24 |
| FIGURE 15 | Particle Size Distribution on S1 .....                                   | 25 |
| FIGURE 16 | Particle Size Distribution on S2 .....                                   | 26 |
| FIGURE 17 | Particle Size Distribution on S3 .....                                   | 26 |
| FIGURE 18 | Particle Size Distribution on S4 .....                                   | 27 |
| FIGURE 19 | Average Particles Size Distribution on SiO <sub>2</sub> Sphere.....      | 27 |
| FIGURE 20 | Agglomeration of Metal Nanoparticles in S1 .....                         | 28 |
| FIGURE 21 | Bare SiO <sub>2</sub> sphere in S2.....                                  | 29 |
| FIGURE 22 | TPR Result for (a),(b),(c),(d) .....                                     | 30 |
| FIGURE 23 | Percentage of CO Conversion at Different Composition.....                | 32 |
| FIGURE 24 | Percentage of CH <sub>4</sub> Selectivity at Different Composition.....  | 32 |
| FIGURE 25 | Percentage of C <sub>5+</sub> Selectivity at Different Composition ..... | 33 |
| FIGURE 26 | FESEM image on 100Co/SiO <sub>2</sub> .....                              | 51 |
| FIGURE 27 | Spectrum Processing on 100Co/SiO <sub>2</sub> .....                      | 51 |
| FIGURE 28 | FESEM image on 95Co5Mn/SiO <sub>2</sub> .....                            | 52 |
| FIGURE 29 | Spectrum Processing on 95Co5Mn/SiO <sub>2</sub> .....                    | 52 |

## LIST OF TABLES

|          |  |    |
|----------|--|----|
| TABLE 1  | List of Chemicals and Equipments ..... | 13 |
| TABLE 2  | Composition of Nanocatalyst .....      | 14 |
| TABLE 3  | Specification for Microreactor .....   | 17 |
| TABLE 4  | Reaction Condition.....                | 19 |
| TABLE 5  | Nanocatalyst Composition .....         | 22 |
| TABLE 6  | Reduction Temperature for TPR.....     | 30 |
| TABLE 7  | Reaction Result .....                  | 31 |
| TABLE 8  | Metal Composition.....                 | 40 |
| TABLE 9  | Appropriate Amount of Metal 43.....    | 43 |
| TABLE 10 | Amount of Water of Metal.....          | 46 |
| TABLE 11 | Amount of Hydrazine vs. Co/Mn.....     | 48 |



# CHAPTER 1

## INTRODUCTION

### 1.1 BACKGROUND STUDY

This project aims to synthesize well-dispersed bimetallic Co/Mn nanocatalyst supported on silica for application in Fischer-Tropsch (FT) reaction. FT technology provides an alternative route to produce fuels and chemicals from sources other than crude oil such as coal, gas or biomass. At present, FT industries employ monometallic nanocatalyst such as iron or cobalt supported on  $\text{SiO}_2$  or  $\text{Al}_2\text{O}_3$ . The problem associated with the traditional oxide supports ( $\text{SiO}_2$  or  $\text{Al}_2\text{O}_3$ ) is that during preparation or catalytic reaction, it often results in the formation of mixed compounds that are responsible for the low dispersions of the metal on these traditional oxide supports. In order to improve the FT process economics for the Co-based nanocatalyst system, significant improvements on the metal dispersion and the particle size distribution of cobalt on the nanocatalyst support are desired. The choice of nanocatalyst preparation route is important in producing small, well-dispersed nanoparticles with narrow particle size range. This project uses the reverse microemulsion (ME) methods to synthesize bimetallic Co/Mn nanocatalyst on silica support. The effect of incorporation of manganese as the second metal in the bimetallic nanocatalyst formulation will be investigated. The second metal could result in electronic and geometrical modifications of the Co/Mn system. The optimization of this synthesis route should lead to well-dispersed and narrow-range cobalt-based nanocatalyst which should result in synergic improvement on FT catalytic activity.

## **1.2 PROBLEM STATEMENT**

The high price of worldwide fuel and dwindling reserve of crude oil has led to the development of a process called Fischer-Tropsch (FT) reaction. This process generates the hydrocarbon product from the synthesis gas mainly hydrogen and carbon monoxide as the raw material for the process. The process is well-known as the alternative process to produce liquid hydrocarbon from natural gas which is cleaner and lack of harmful substances as byproducts. Catalyst is very important in FT reaction in order to gain better performance of reaction and to reduce the selectivity of undesired hydrocarbon product ( $\text{CH}_4$ ) and increase the selectivity of desired hydrocarbon product ( $>\text{C}_{5+}$ ).

The reverse microemulsion method has been proposed to produce the bimetallic nanocatalyst for the FT reaction. Based on the earlier research studies, this method produced the better result compared to other catalyst preparation method such as impregnation method in terms of metal dispersion, surface area and particle size. Moreover, the current experimental practices on reverse microemulsion method only focus on the production of a nanocatalyst containing monometallic either Co or Mn. Therefore, this research project is aim to produce the high performance bimetallic nanocatalyst via reverse microemulsion method which has high number of active site, easily reducible and well-dispersed metal particles. The properties of bimetallic nanocatalyst with different compositions of Co and Mn will be studied and the best composition for FT reaction will be determined.

## **1.3 OBJECTIVE OF THE PROJECT**

The objectives of the project are:

1. To synthesize well-dispersed bimetallic nanocatalyst consisting of cobalt-manganese in different composition on silica support via reverse microemulsion method.
2. To characterize and study the properties of the nanocatalyst by applying several characterization methods which are Transmission Electron

Microscopy (TEM), Field Emission Scanning Electron Microscopy (FESEM) and Temperature Programmed Reduction (TPR).

3. To evaluate the performance of the nanocatalyst in a Fischer-Tropsch reaction.

#### **1.4 SCOPE OF STUDY**

The scopes of study of the project are:

1. Setting up a laboratory scale experiment to prepare Co/Mn nanocatalyst by reverse microemulsion method on silica dioxide (SiO<sub>2</sub>) support.
2. Studying the effects of different composition of manganese and cobalt.
3. Characterization of nanocatalysts using Transmission Electron Microscopy (TEM), Field Emission Scanning Electron Microscopy (FESEM) and Temperature Programmed Reduction (TPR).
4. Performance evaluation of these nanocatalysts.

#### **1.5 RELEVANCY OF THE PROJECT**

In synthesis and characterization of bimetallic nanocatalyst, the right choice of preparation route is required in order to produce the desired nanocatalyst and meet the project objective. The main objective of this project is to synthesize the well-dispersed Co/Mn bimetallic nanocatalyst by using reverse microemulsion method and to study its properties through several characterization methods. The cobalt-based nanocatalyst is chosen since the interest has shifted to cobalt-based nanocatalyst for Fischer-Tropsch (FT) reaction replacing the Iron (Fe) in the first place (Y. Zhang, 2007). Manganese also is a promoter with particular interest to be used in producing the bimetallic nanocatalyst (den Breejen, 2011). The characterization of bimetallic nanocatalyst will be conducted in the centralized analytical laboratory. When manganese is added to the cobalt, the metal dispersion is expected to be greater and narrow particle size distribution will be achieved as well as better performance of the nanocatalyst in the FT reaction. This project is relevant

since the current interest for combination of cobalt and manganese is increasing and this combination might produce the better catalyst for FT and contribute to the research and development (R&D) of this field.

## **1.6 FEASIBILITY OF THE PROJECT**

The reverse microemulsion method is the experimental work and need to be done in laboratory as there are available tools, equipment and chemicals which are the main elements for this project and as an indicator to determine whether this project might successful or not. The time given to conduct the experiment is also sufficient and reasonable which include preparation of preparing nanocatalyst until testing of the catalyst in the microreactor for Fischer-Tropsch reaction.

The student was given 29 weeks effective from 14<sup>th</sup> January 2013 to attach under Dr. Rashidah binti Mohd Pilus, Fundamental and Applied Sciences Department, Universiti Teknologi PETRONAS and Dr. Noor Asmawati binti Mohd Zabidi, Centralized Analytical Department, Universiti Teknologi PETRONAS. Based on the knowledge in project management, the student has developed a well and organized Gantt's chart to conduct the project (refer methodology). By having regular formal and informal meetings and discussions with the supervisor, co-supervisor and other lecturers, it helps the student to gather as much information on conducting the project.

As a conclusion, Gantt's chart and regular informal discussion will ensure the project to be on track and fulfill the objectives.

## **CHAPTER 2**

### **LITERATURE REVIEW**

#### **2.1 INTRODUCTION TO FISCHER-TROPSCH TECHNOLOGY**

The Fischer-Tropsch technology was invented in Germany in early 1920s whereas at that time Germany is the petroleum-poor but coal-rich country. Franz Fisher and Hans Tropsch from Kaiser Wilhelm Institute was the inventor for the original Fischer-Tropsch process. It was used by Germany and Japan during World War II to produce alternative fuels. Germany's annual synthetic fuel production can reached 124,000 barrels per day in 1994 which the produce in 25 plants in the country (U.S Department of Energy, 2006).

The brief description of Fischer-Tropsch technology is the process used to convert synthesis gas containing hydrogen ( $H_2$ ) and carbon monoxide (CO) to produce hydrocarbon (HC) products. The hydrocarbon product can be in the form of liquid, gaseous and solid form but most of the product is in the liquid form at ambient temperature and pressure. The process also produces the oxygenated hydrocarbon as the byproduct. The example of oxygenated hydrocarbon produced from the reaction is alcohols but exclude the methanol in the formation (Steynberg, 2004, p. 1-163).

Nowadays, Fischer-Tropsch reaction is the technology which converts coal, natural gas, and low-refinery products into a high-value and clean burning fuel. Some advantages of FT hydrocarbons compared to crude oil as a feedstock for fuel production are the absence of sulfur, nitrogen or heavy metal contaminants, and the low aromatic content (Steynberg, 2004). Another advantage is the resultant fuel is virtually interchangeable with conventional diesel fuels and can be blended with diesel at any ratio with little to no modification. In terms of product produced, Fischer-Tropsch fuels offer important emissions benefits compared with diesel,

reducing nitrogen oxide, carbon dioxide, and particulate matter (United States Environmental Protection Agency, 2002).

## 2.2 FISCHER-TROPSCH PRODUCT DISTRIBUTION

The Fischer-Tropsch process uses syngas as the feedstock which is the mixture of hydrogen (H<sub>2</sub>) and carbon monoxide (CO) with different H<sub>2</sub>:CO ratios to produce hydrocarbon (HC) product. The basic equation for the process is as follow:



The Fischer-Tropsch process produces hydrocarbon as well as another byproduct in the reaction as the undesired reaction. The original Fischer-Tropsch process is described by the following chemical equation:



The initial Fischer-Tropsch reactants in the above reaction which are CO and H<sub>2</sub> can be produced by other reactions such as the partial combustion of a hydrocarbon or by the gasification of coal or biomass. The chemical equation is as follow:



Fischer-Tropsch reactants can also be produced from methane in the gas to liquid process:

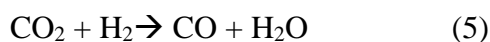


When coal or biomass are used as source, the resulting syngas as the feedstock contains a large amount of carbon dioxide (CO<sub>2</sub>), thus demanding the expensive purification steps (about 5\$/MT CO<sub>2</sub>) which increase significantly the process expenses (Chiesa and Consonni, 2003).

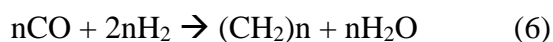
Unlike CO hydrogenation, the understandings of carbon dioxide hydrogenation process still a major challenge. There have been various attempts to transform carbon dioxide into hydrocarbons, mainly using those catalysts that have been proven active in the Fischer-Tropsch process, such as Ni, Ru and Co. Most attempts yielded

methane as the only product, even if water-gas shift active promoters were added (Riedel et al., 1999). It seems likely that carbon dioxide hydrogenation proceeds via a two step reaction mechanism (Lee et al., 1992):

In the first step, carbon dioxide is converted into carbon monoxide through the reverse water-gas shift reaction. The equation for the conversion of carbon dioxide to carbon monoxide through the reverse water-gas shift reaction is as follow:



The reaction is endothermic reaction with  $\Delta H_{573\text{ K}}^0 = 38 \text{ kJ mol}^{-1}$ . The carbon monoxide from the first reaction reacts according to the Fischer-Tropsch process to produce hydrocarbon.



The reaction release the heat due to exothermic reaction  $\Delta_R H_{573\text{ K}}^0 = -166 \text{ kJ mol}^{-1}$  (Herranz et al., 2006, p. 66).

The spread in carbon number products can be varied by manipulating the operating temperature, the type of catalyst, the amount or type of promoter present, the feed gas composition, the operating pressure, or the type of reactor used.

### 2.3 CATALYST FOR FISCHER-TROPSCH SYNTHESIS

Transition metal oxides are generally the good hydrogenation catalyst. The specific activity of various Group VIII metals are determined to observed their reactivity towards Fischer-Tropsch reaction. The test conducted by Vannice (Vannice, 1975) give the trend of the result of  $\text{Ru} > \text{Fe} > \text{Ni} > \text{Co} > \text{Rh} > \text{Pd} > \text{Pt}$  although the average hydrocarbon molecular weight decrease in order  $\text{Ru} > \text{Fe} > \text{Co} > \text{Rh} > \text{Ni} > \text{Ir} > \text{Pt} > \text{Pd}$ . Based on the order, the cheap Fe catalyst have the high potential to contribute in the Fischer-Tropsch reaction. Co-based catalyst were later preferred simply because the requirement for operating pressure is milder compared to the high pressure reactor for Fe catalyst. In the positive side, Fe readily forms oxides,

carbides, nitrides and carbonitrides which are also active for Fischer-Tropsch reaction. Another advantages of Fe is the stronger tendency compared to Co or Ni in order to produce elemental carbon which can deactivate the catalyst. The formation of Co and Ni is thermodynamically unfavoured at Fischer-Tropsch reaction since the lower temperature use for the reaction (433-573 K). The reaction would only apply for process carried out at the temperature more than 673 K and some other relatively severe condition that favour the reaction (Herranz et al., 2006, p. 67). Ru may become active as low as 373 K which led to the production of high molecular weight of hydrocarbon. Carbide of Ru is unknown at typical Fischer-Tropsch condition. The metal which is not in the group VIII metal, Mo also can exhibit the moderate Fischer-Tropsch activity and carbide of Mo show excellent alkene production rate. Mo also have the special properties which is sulphur-resistance characteristic. Other metal from Group VIII comprised Rh, Re, Os, Pd, Pt and Ir yield mostly oxygenated compounds partly because CO does not chemisorb dissociatively on these metals (Adesina, 1995).

It is proven in some of the previous study that the presence of two or more metals often leads to better Fischer-Tropsch catalyst. Currently, the bimetallic catalyst has been used for the steam reforming operations. Then, the highly potential and quality of bimetallic catalyst has lead it to be use in the Fischer-Tropsch reaction. The objective of bimetallic formulation is to take advantage of possible synergetic effect between the two metals and thus, produce highly active, selective and stable catalysts. Moreover, in the industrial application, bimetallic catalyst exhibit superior stability compared to monometallic catalysts. Study by Duvenhage et al (1997) indicates that the addition of small amount of Co to Fe could influence the Fe catalyst dramatically. Fe-Mn catalyst is another example of bimetallic catalyst that is widely used in the Fischer-Tropsch reaction.

## **2.4 REVERSE MICROEMULSION METHOD**

Microemulsion can be in the form of homogeneous in macroscale or microheterogeneous in nanoscale dispersion in two immiscible liquids containing the nanosized particle as the domain of one or two liquids in the other. The interfacial



film of surface active molecules acts as the stabilizer in the liquid. The difference between normal emulsion and microemulsion is the particle size and stability. The properties of microemulsion are as follows (Zielinska-Jurek, 2012, p. 229).

- Thermodynamically stable
- Single optically isotropic
- Spontaneous
- Ultralow interfacial tension of oil and water
- Large interfacial area
- Large capacity to solubilize both aqueous and oil-soluble compounds

Depending on the proportion of various components and hydrophilic-lipophilic balance (HLB) value of used surfactant in microemulsion can be classified as water-in-oil (w/o), oil-in-water (o/w) and the intermediate bicontinuous structural types that can turn reversibly from one type to the other. The dispersed phase consists of monodispersed droplets in the size range of 5-100 nm. The nanodroplet size can be modified by varying droplet concerned parameters such as the type of stabilizer, continuous phase, the precursor content dissolved within the nanodroplet, and the water content, referred to as molar ratio of water to surfactant ( $w$ ). In addition the stability of the microemulsion can be influenced by addition of salt, concentration of reagent, temperature or pressure (Zielinska-Jurek, 2012, p. 229).

The preparation of bimetallic nanoparticles in water-in-oil microemulsion commonly consists of metallic salt and reducing agent. The **FIGURE 1** is the schematic diagram for the process of microemulsion technique (Zielinska-Jurek, 2012, p. 230).

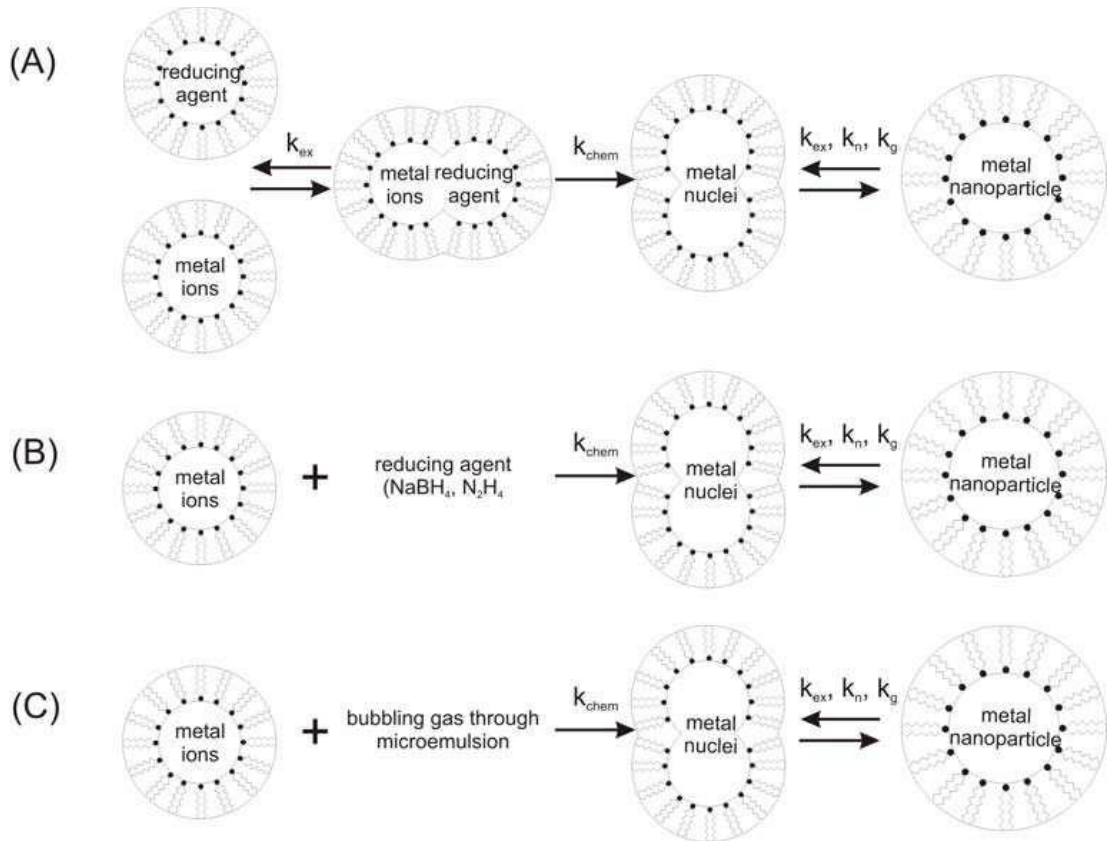


FIGURE 1. Nanoparticles preparation using microemulsion technique

There are some of the constant which involves in the microemulsion technique above.  $k_{chem}$  is the rate constant for chemical reaction,  $k_{ex}$  is the rate constant for intermicellar exchange dynamics,  $k_n$  is the rate constant for nucleation, and  $k_g$  is the rate constant for particle growth. For the process description, the two microemulsion is mix up and the exchange of reactants between micelles takes place which occur after the mixing of two microemulsion was done. The Brownian motion, the attractive Van Der Waals forces and repulsive osmotic forces between reverse micelles caused the collision of water droplets and at the same time the exchange of reactants between micelles occur as stated earlier. Successful collisions give the result of coalescence, fusion, and efficient mixing of the reactants. The reaction between the initial stage of the particle and after the particle is soluble result in the formation of metal nuclei. At the initial stage of the nucleation, metal salt is reduced to give zerovalent metal atoms, which can collide further with metal ions, metal atoms, or cluster to form an irreversible seed of stable metal nuclei. The growth initiate around the nucleation point where successful collision occurs between a reverse micelle carrying a nucleus and another one carrying the product monomers

with a coming of more reactants due to intermicellar exchange. The nucleation reaction and particle growth occur within the micelles while the size and morphology of nanoparticles product depend on the size and shape of the nanodroplets and the type of surfactant. The surface of the particles attached on the surfactant molecule in order to stabilize and prevent the particle to growing further (Zielinska-Jurek, 2012, p.230-231).

The method (A) in the schematic diagram above is the preparation of bimetallic nanoparticles which is the combination of two metal ions in the two microemulsions. For a single microemulsion the preparation method are shown in (B) and (C). A precursor of metal particles which act as one of the reactant is solubilised inside reverse micelles. The second reactant which is a reducing agent is added directly to the microemulsion system. For the formation of nanoparticles formed in the single microemulsions, the mechanism is based on intramicellar nucleation growth and particle aggregation (Zielinska-Jurek, 2012, p. 231-232). However, the bimetallic nanoparticles managed to attract the interest for the further research and study due to its unique catalytic, electronic, and optical properties. The structure of bimetallic combinations depends on the preparation conditions, miscibility, and kinetics of the reduction of metal ions.

## CHAPTER 3

### METHODOLOGY

#### 3.1 PROJECT ACTIVITIES

The methodology for conducting this project is by experimental methods. As this project is mainly in the field of research and development (R&D), the results obtained from this research can be used to compare with other literature with similar scope of study. Besides, the result in terms of reactivity towards the Fischer-Tropsch (FT) reaction obtained from this research using different composition of Co/Mn nanocatalyst can be used as a basis of comparison with other studies. The **FIGURE 2** shows the general experimental procedures that were implemented in this research project.

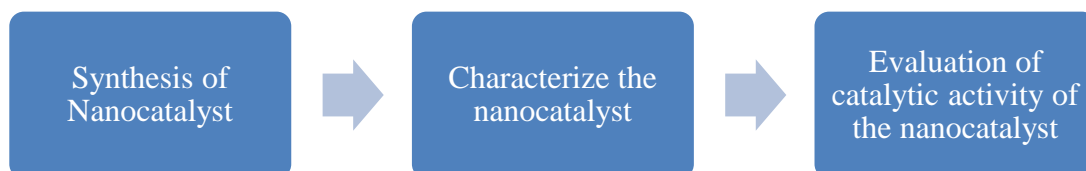


FIGURE 2. The schematic diagram of research project activities

#### 3.2 EQUIPMENTS AND CHEMICALS

In the experiments that are going to be conducted, several equipment and chemicals are needed to prepare the nanocatalyst from reverse microemulsion method. List of the equipment and chemical used in this research study is given in the **TABLE 1**.

TABLE 1. List of Chemicals and Equipments

| Chemicals/Equipment  | Supplier/Model   | Purity (%) | Amount  | Purpose  |
|--|------------------|------------|---|--|
| Silica Dioxide sphere (SiO <sub>2</sub> )  | Evonik           | 99.8       | <ul style="list-style-type: none"> <li>• 3-4 g (5 samples)</li> <li>• 300 mg (4 tests)</li> </ul> | Catalyst support   |
| Triton X-114   | Aldrich          | 98.0       | 60.0 g  | Surfactant   |
| Cyclohexane (C <sub>6</sub> H <sub>12</sub> )  | Aldrich          | 99.5       | 500 ml  | Surfactant oil phase   |
| Co(NO <sub>3</sub> ) <sub>2</sub> .6H <sub>2</sub> O   | Merck            | 98.5       | 2.0 g   | Catalyst Precursor   |
| Mn(NO <sub>3</sub> ) <sub>2</sub> .6H <sub>2</sub> O   | Merck            | 98.5       | 2.0 g   | Catalyst Precursor   |
| Hydrazine (N <sub>2</sub> H <sub>4</sub> )   | Aldrich          | 98.0       | 2.0 g   | Reducing agent   |
| Tetrahydrofurane   | Merck            | 99.5       | 550 ml  | Emulsion destabilizing agent                                   |
| Ethanol  | Merck            | 95.0       | 1 L   | Washing  |
| Whatman® Filtration Paper or membrane filter.<br>(For membrane filter, pore size : 0.2 µm<br>Diameter :47 nm | Whatman®         | -          | 5 pieces  | Filtrate the solid sample of nanocatalyst                      |
| Field Emission Scanning Electron Microscopy (FESEM)  | Gemini           | -          | 0.2 g of nanocatalyst for all test  | Observe morphology of nanocatalyst                             |
| Transmission Electron Microscopy (TEM)   | Zeis Libra 200FE | -          | 0.2 g of nanocatalyst for all test  | Observe morphology of nanocatalyst (higher resolution)         |
| Temperature Programmed Reduction (TPR)   | Thermo Electron  | -          | 2 g of nanocatalyst for each test   | Identify most efficient reduction temperature for nanocatalyst |

|   |                 |   |  |                                    |
|---|-----------------|---|--|------------------------------------|
| Stainless Steel Fixed Bed<br>Microreactor | PID<br>Eng&Tech | - | 0.03 g<br>nanocatalyst<br>for each<br>reaction | Nanocatalyst<br>catalytic reaction |
|---|-----------------|---|--|------------------------------------|

### 3.3 PREPARATION OF Co/Mn NANOCATALYST

The methodology of nanocatalyst preparation for laboratory scale production through the reverse microemulsion method is explained in the procedure below:

- Five (5) samples of different composition of Co/Mn including the pure Co and pure Mn were prepared by using aqueous cobalt nitrate  $\text{Co}(\text{NO}_3)_2 \cdot 6\text{H}_2\text{O}$  (Merck) and manganese nitrate  $\text{Mn}(\text{NO}_3)_2 \cdot 6\text{H}_2\text{O}$  (Merck) as shown in the **TABLE 2**.

TABLE 2. Composition of Nanocatalyst

| No of Sample | Composition of Co:Mn (mol %) | Composition of Co:Mn (10wt %) | Mass of Co Nitrate (g) | Mass of Mn Nitrate (g) | Mass of water (g) | Mass of hydrazine (g) | Mass of Triton (g) | Mass of $\text{C}_6\text{H}_{12}$ (ml) |
|--------------|------------------------------|-------------------------------|------------------------|------------------------|-------------------|-----------------------|--------------------|--|
| 1            | 100:0                        | 100:0                         | 0.25                   | -                      | 0.99              | 0.2564                | 11.175             | 100                                    |
| 2            | 95:5                         | 95.3:4.7                      | 0.24                   | 0.0104                 | 0.988             | 0.2692                | 11.175             | 100                                    |
| 3            | 87.5:12.5                    | 88.2:11.8                     | 0.22                   | 0.031                  | 0.987             | 0.2596                | 11.175             | 100                                    |
| 4            | 75:25                        | 76.3:23.7                     | 0.19                   | 0.063                  | 0.986             | 0.2628                | 11.175             | 100                                    |
| 5            | 0:100                        | 0:100                         | -                      | 0.26                   | 0.98              | 0.2885                | 11.175             | 100                                    |

All the calculations steps are shown in **APPENDIX 1**

- Silica dioxide ( $\text{SiO}_2$ ) was dried at 120 °C for 6 hours.
- Prepared microemulsion A consisting of nonionic surfactant Triton X-114 and cyclohexene ( $\text{C}_6\text{H}_{12}$ ). 11.175 g (0.02 mol) of Triton X-114 was poured into 100 ml volumetric flask and topped up with cyclohexene until reached the mark.
- Prepared microemulsion B consisting of 0.24 g ( $8.25 \times 10^{-4}$  mol)  $\text{Co}(\text{NO}_3)_2 \cdot 6\text{H}_2\text{O}$  and 0.0104 g ( $3.62 \times 10^{-5}$  mol)  $\text{Mn}(\text{NO}_3)_2 \cdot 6\text{H}_2\text{O}$  for sample 2. For other samples, the components were adjusted accordingly.

5. Transferred microemulsion A into two-neck round bottom flask.
6. Purged microemulsion A with nitrogen ( $N_2$ ) and stirred. FIGURE 3 shows the synthesis setup in the laboratory.



FIGURE 3.Synthesis Setup

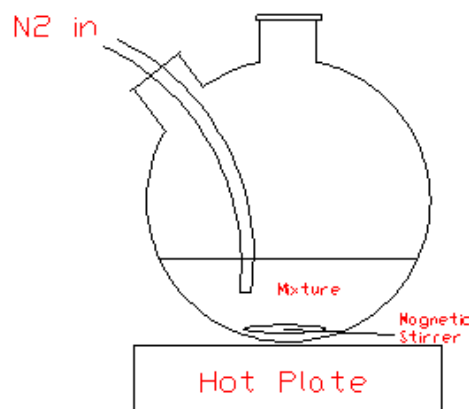


FIGURE 4.Synthesis Setup  
Schematic Drawing

7. Poured microemulsion B into stirred solution A. The mixture is stirred vigorously until the formation of microemulsion mixture appeared and can be seen approximately after 15 minutes of stirring.
8. After about 15 minutes, the mixture became cloudy and turned off white.
9. 0.2692 g ( $8.40 \times 10^{-3}$  mol) hydrazine was added then 0.45 g ( $7.50 \times 10^{-3}$  mol) of dried  $SiO_2$  was added into the stirred mixture.
10. The mixture was stirred for 3 hours while the dropwise of tetrahydrofuran (THF) was added at 1 ml/min using syringe. The rapid addition of THF could result a fast agglomeration and uncontrolled particle deposition on the support.



FIGURE 5.Syringe

11. The mixture was left overnight for sedimentation process. The particle sediment slowly at the bottom of the two necks round bottom flask.
12. The solid nanocatalyst was collected by using vacuum filtration. Wash the nanocatalyst several times with ethanol.
13. The nanocatalyst was dried overnight at 120 °C.
14. Remaining traces of surfactant and nitrates precursor were removed by calcining the nanocatalyst under nitrogen flow at 500 °C for 3 hours. The nanocatalyst was then cooled in nitrogen (N<sub>2</sub>) flow.

### **3.4 CHARACTERIZATION METHOD OF NANOCATALYST**

The nanocatalyst produced from the reverse microemulsion usually in the form of microheterogeneous catalysts which are the metal particles attached on the support. The support used in this study is silica dioxide (SiO<sub>2</sub>). The size of metal particle plays an important role for the nanocatalyst efficiency, where the main properties that need to characterize and determine is the metal dispersion on the support and size distribution of the nanocatalyst. There are several methods to characterize the nanocatalyst produced from reverse microemulsion synthesis. Listed below are the characterization methods that are used to analyze the sample of nanocatalyst.

#### **3.3.1 Transmission Electron Microscopy (TEM)**

The sample for TEM analysis was prepared by taking a small amount of nanocatalyst which was about 0.05 g and transferred it into vial. Poured the acetone solution about 1/3 of the vial as a solvent. The sample was sonicated 1 hour. The sample was further prepared by using dimple grinding. Then, the sample was ready for TEM analysis. 100 KX magnification was used for the analysis and the images was taken at different ranges of scale which are 50 nm and 100 nm depending on morphology of the sample.



### 3.3.2 Field Emission Scanning Electron Microscopy (FESEM)

The small amount of nanocatalyst powder which was about 0.05 g was sprinkled on double-sided carbon tape and placed on sample stub for FESEM analysis. 50 KX magnification was used for the FESEM analysis with the image scale of 200nm.

### 3.3.3 Temperature Programmed Reduction (TPR)

0.15 g nanocatalyst sample was used for TPR. The analysis started at the room temperature 30 °C. The TPR yields quantitative information of the reducibility of the oxide's surface, as well as the heterogeneity of the reducible surface for the all samples of nanocatalyst. The reducing gas mixture (typically 3% to 17% hydrogen diluted in argon or nitrogen) was used to flows over the sample. A thermal conductivity detector (TCD) is used to measure changes in the thermal conductivity of the gas stream

## 3.5 MICROREACTOR STUDY

The research project was used MICROACTIVITY-Reference equipment to study the performance of bimetallic nanocatalyst in Fischer-Tropsch (FT) reaction. The MICROACTIVITY-Reference is an automatic and computerized laboratory reactor for reactions of catalytic microactivity with reactor bypass, preheater evaporator, pressure control valve and other process layouts in hot box, which avoids the possible condensation of volatile products, at the time that preheats the reactants efficiently. **TABLE 3** shows the specification of the microreactor.

TABLE 3. Specification for Microreactor

| Equipment                 | Microactivity-Reference |
|---------------------------|-------------------------|
| Voltage                   | 230 VAC ( $\pm 5\%$ )   |
| Frequency                 | 50 Hz ( $\pm 1\%$ )     |
| Maximum Power Consumption | 2000 W                  |
| Protection                | 10 A circuit breaker    |

|   |                           |
|---|---------------------------|
| Maximum power consumption of furnace    | 80 W                      |
| Maximum power consumption of furnace    | 4 heaters of 165 W        |
| Ambient Temperature range for operating | 5-40°C                    |
| Ambient Temperature range for storing   | 20-70°C                   |
| Recommended humidity range              | 5-80 %                    |
| Dimension, cm (height x width x depth)  | 70 x 60 x 55 9 basic unit |

**FIGURE 6** show the microreactor assembling while **FIGURE 7** show the step of nanocatalyst loading before the reaction start.

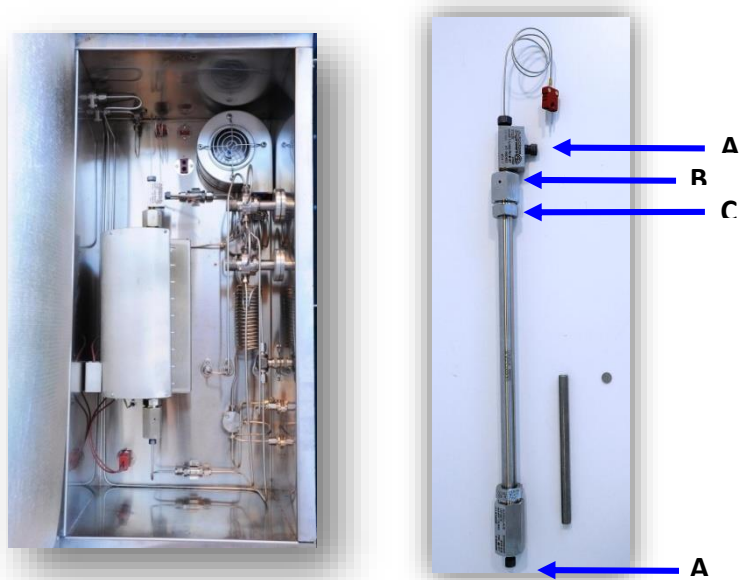


FIGURE 6. Microreactor Assembling

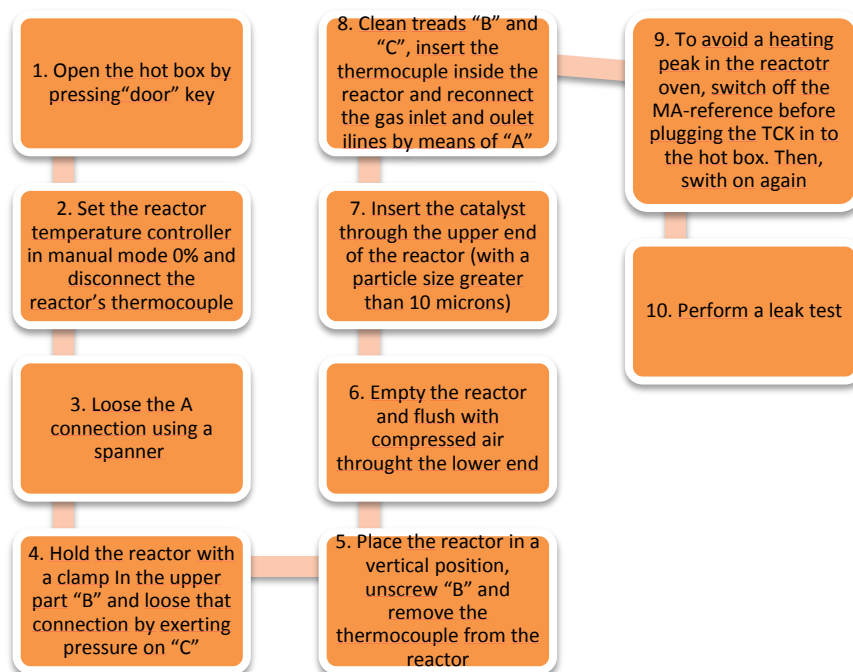


FIGURE 7. Catalyst Load Steps

Then, proceed with the reaction. The parameters used for the reaction are shown in the **TABLE 4**.

TABLE 4. Reaction Condition

| Sample                    | Mass (mg) | Flow rate of CO or H <sub>2</sub> ( $\frac{\text{L}}{\text{gcat. hour}}$ ) | Reduction Temperature (set 1) (°C) in H <sub>2</sub> flow | Reduction Temperature (set 2) (°C) in H <sub>2</sub> flow | Reaction Temperature (°C) | Pressure (bar) |
|---------------------------|-----------|--|---|---|---------------------------|----------------|
| 100Co/SiO <sub>2</sub>    | 30        | 12   | 370   | 400   | 220                       | 10             |
| 95Co5Mn/SiO <sub>2</sub>  | 30        | 12   | 370   | 400   | 220                       | 10             |
| 88Co12Mn/SiO <sub>2</sub> | 30        | 12   | 370   | 400   | 220                       | 10             |
| 76Co24Mn/SiO <sub>2</sub> | 30        | 12   | 370   | 400   | 220                       | 10             |

The performance of this catalyst in a Fischer-Tropsch (FT) reaction was evaluated in a fixed-bed stainless steel microreactor at 10 bar, 220 °C and H<sub>2</sub>:CO at 2:1 ratio. The catalyst was reduced at two reduction temperatures of 370 °C or 400 °C, prior to reaction. The product was analyzed via on-line gas chromatograph (GC) to identify the product from the microreactor. Output from the GC was used to calculate the

percentage of carbon monoxide (CO) and selectivity of hydrocarbon (HC). The percentage of CO conversion, methane (CH<sub>4</sub>) selectivity and C<sub>5+</sub> selectivity is calculated by using formula (7), (8) and (9).

$$\text{CO conversion (\%)} = \frac{\text{CO}_{\text{in}} - \text{CO}_{\text{out}}}{\text{CO}_{\text{in}}} \times 100 \quad (7)$$

$$\text{CH}_4 \text{ selectivity (\%)} = \frac{\text{Moles of CH}_4}{\text{Total moles of hydrocarbon}} \times 100 \quad (8)$$

$$\text{C}_5^+ \text{ selectivity (\%)} = \frac{\text{Moles of C}_5^+}{\text{Total moles of hydrocarbon}} \times 100 \quad (9)$$

**FIGURE 8** shows the MICROACTIVITY-References equipment connected to the GC in the laboratory. The schematic diagram of microreactor is shown in **APPENDIX 5**.



**FIGURE 8.** MICROACTIVITY-References connected to GC

### 3.6 PROJECT FLOW

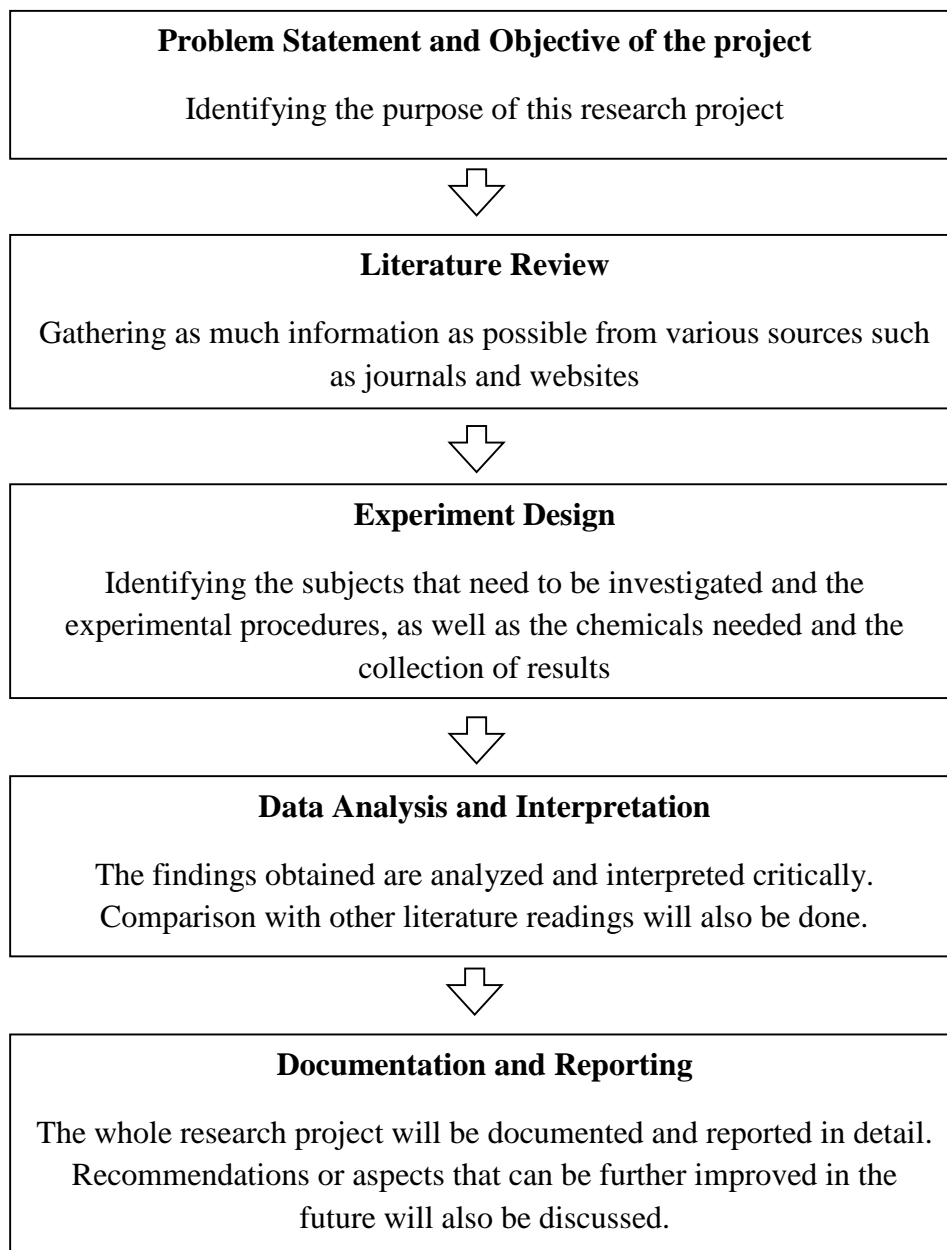


FIGURE 9. Project Flow for the Research Project

### 3.7 KEY MILESTONES/GANTT'S CHART

Key Milestones and Gantt's Chart are attached on **APPENDIX 2** and **APPENDIX 3**.

## CHAPTER 4

### RESULT AND DISCUSSION

#### 4.1 CATALYST FORMULATION

Five compositions were prepared based on calculations shown in the **APPENDIX 1**. **TABLE 5** shows the five different compositions of nanocatalyst.

TABLE 5. Nanocatalyst Composition

| Sample Code | Composition               |
|-------------|---------------------------|
| S1          | 100Co/SiO <sub>2</sub>    |
| S2          | 95Co5Mn/SiO <sub>2</sub>  |
| S3          | 88Co12Mn/SiO <sub>2</sub> |
| S4          | 76Co24Mn/SiO <sub>2</sub> |

#### 4.2 CHARACTERIZATION OF NANOCATALYST

##### 4.2.1 Morphology

TEM images of S1 are shown in **FIGURE 10**. *Image 1* and *Image 2* were taken on the same sample at different locations.

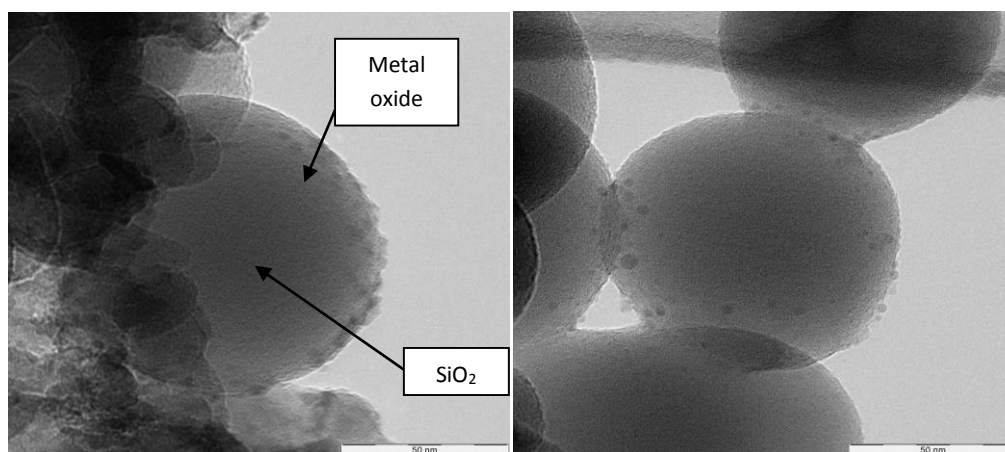


*Image 1*

*Image 2*

FIGURE 10. TEM images of S1 at different location

From the observation of the TEM images, some Co nanoparticles were deposited on SiO<sub>2</sub> sphere but not very uniform as some SiO<sub>2</sub> spheres were still bare.

**FIGURE 11** shows the TEM images for S2 at different location. For S2, most of the SiO<sub>2</sub> spheres were still bare since only some of the metal nanoparticles appeared and deposited on the SiO<sub>2</sub> spheres. The dispersion of metal nanoparticles were not very uniform as the same as S1.

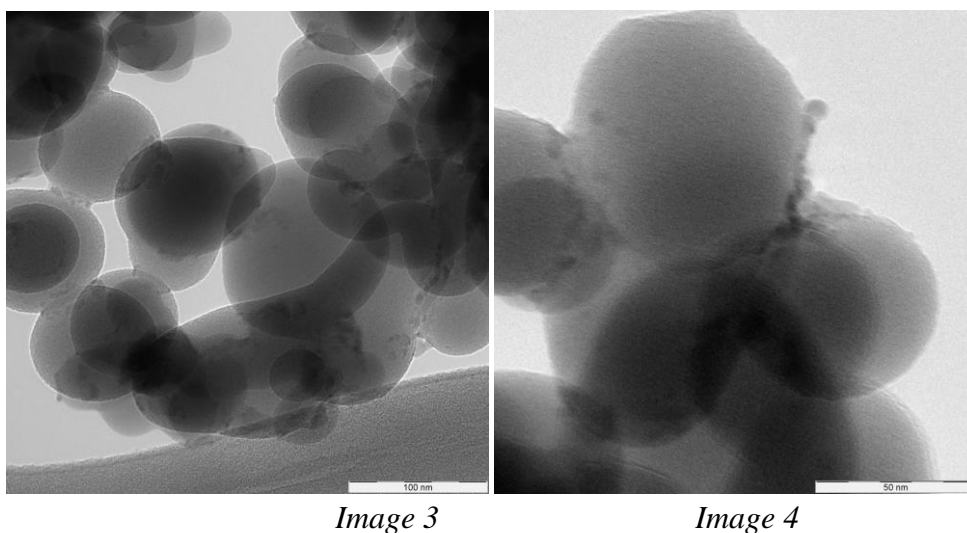


FIGURE 11. TEM images of S2 at different location

**FIGURE 12** shows the TEM images of S3. In this sample, metal nanoparticles look larger and better dispersed on the SiO<sub>2</sub> spheres than those in S2.

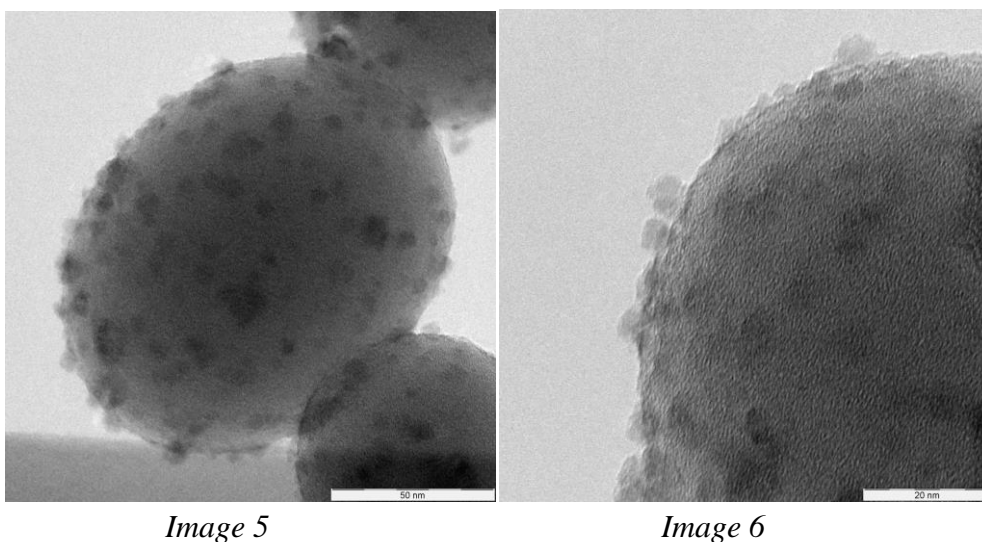
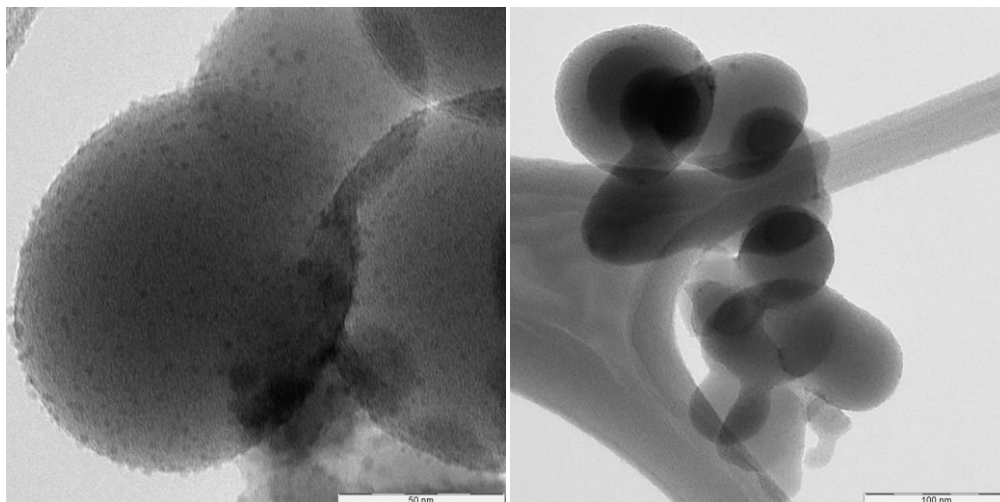


FIGURE 12. TEM images of S3 at different location

**FIGURE 13** show the TEM images of S4 at different location. In this sample, metal nanoparticles deposited on SiO<sub>2</sub> sphere appeared smaller and the metal nanoparticles in S4 were better dispersed compared to those in S3.



*Image 7*

*Image 8*

FIGURE 13. TEM images of S4 at different location

**FIGURE 14** shows the TEM images of sample 5 (S5) consisting of pure Mn supported on silica, 100Mn/SiO<sub>2</sub>. From the TEM images, Mn nanoparticles were not deposited on the entire SiO<sub>2</sub> spheres.

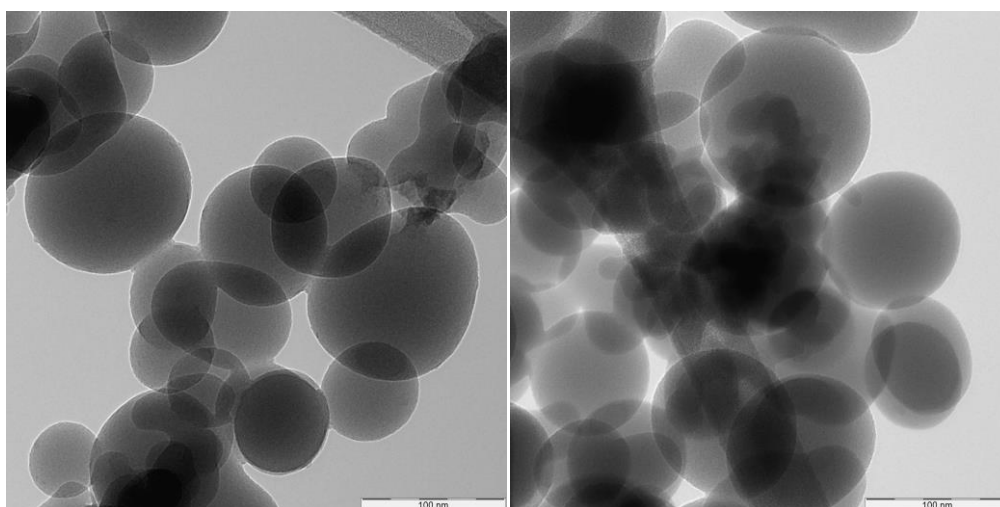


*Image 9*

*Image 10*

FIGURE 14. TEM images of S5 at different location



The main purpose of TEM is to analyze the metal nanoparticles size deposited on the SiO<sub>2</sub> sphere surface area as the support. The images show the particle dispersion and distribution on the support for all nanocatalyst at different location. As being observed from TEM images, most of the particles were distributed on the SiO<sub>2</sub> sphere surface with the range of size between 1.5 nm to 7 nm. The TEM images were analyzed by estimating the size of the nanoparticles. Typically 30-40 nanoparticles were measured for each sample and the result are shown in **FIGURE 15, 16, 17 and 18.**

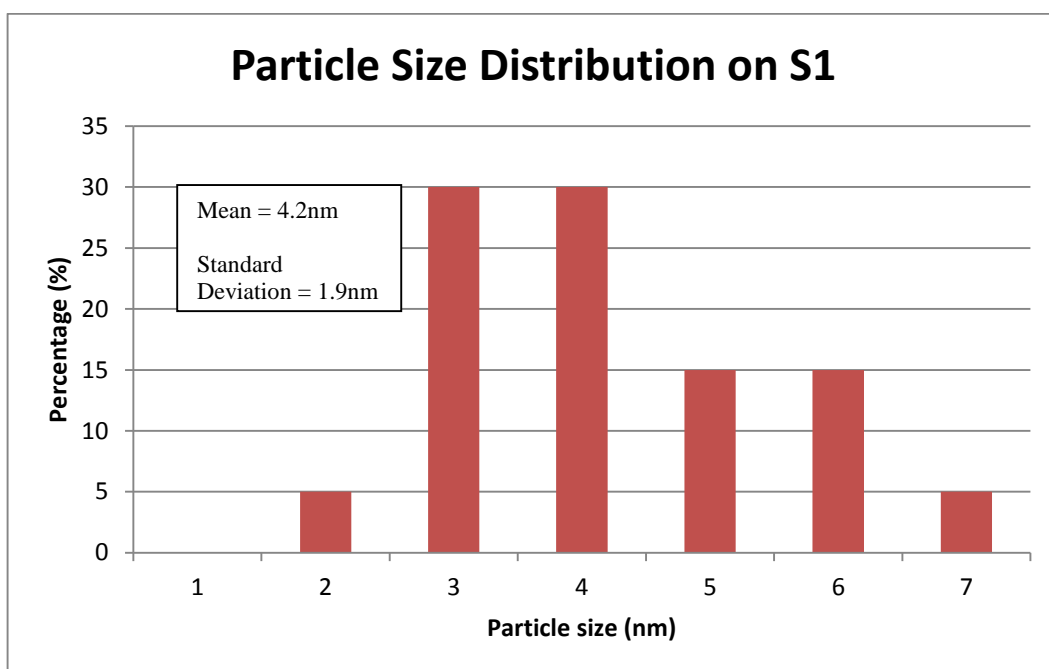


FIGURE 15. Particle Size Distribution on S1

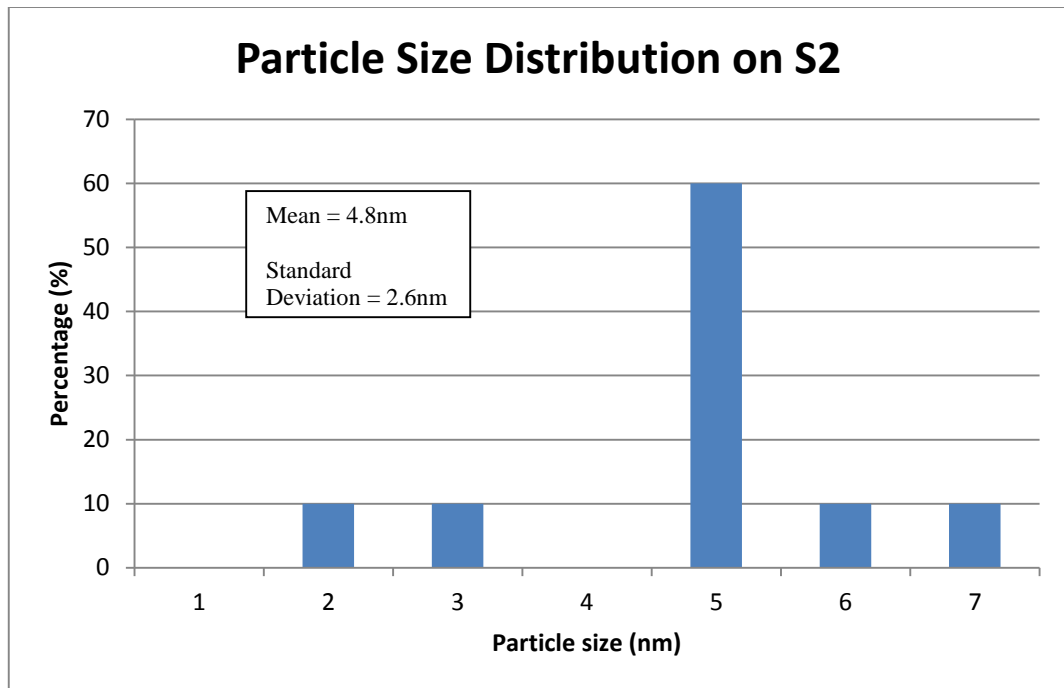


FIGURE 16. Particle Size Distribution on S2

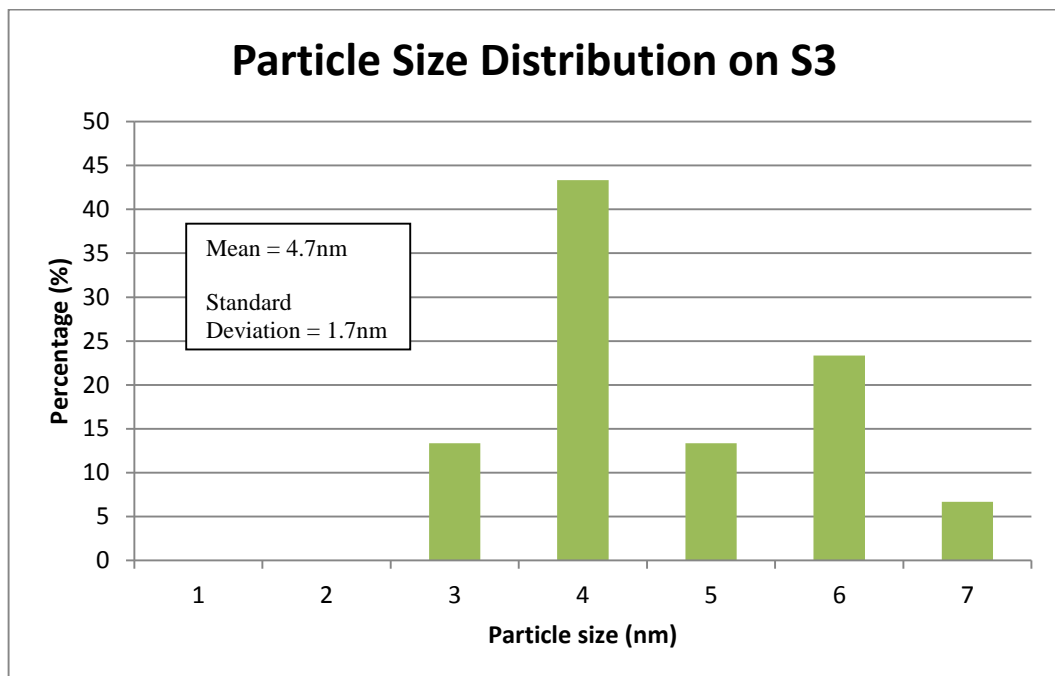


FIGURE 17. Particle Size Distribution on S3

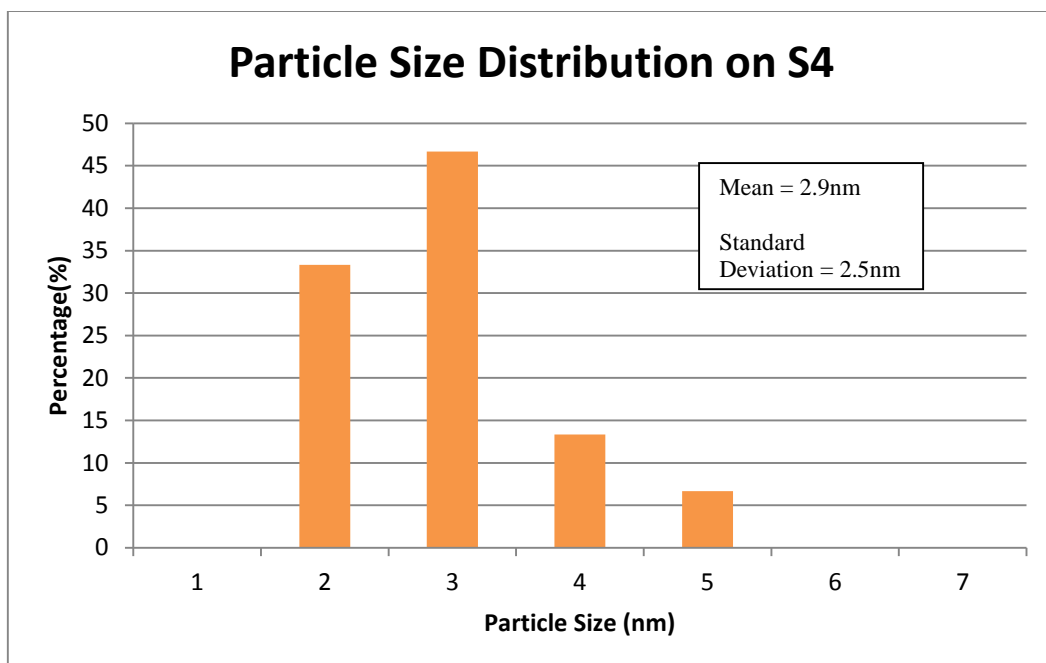


FIGURE 18. Particle Size Distribution on S4

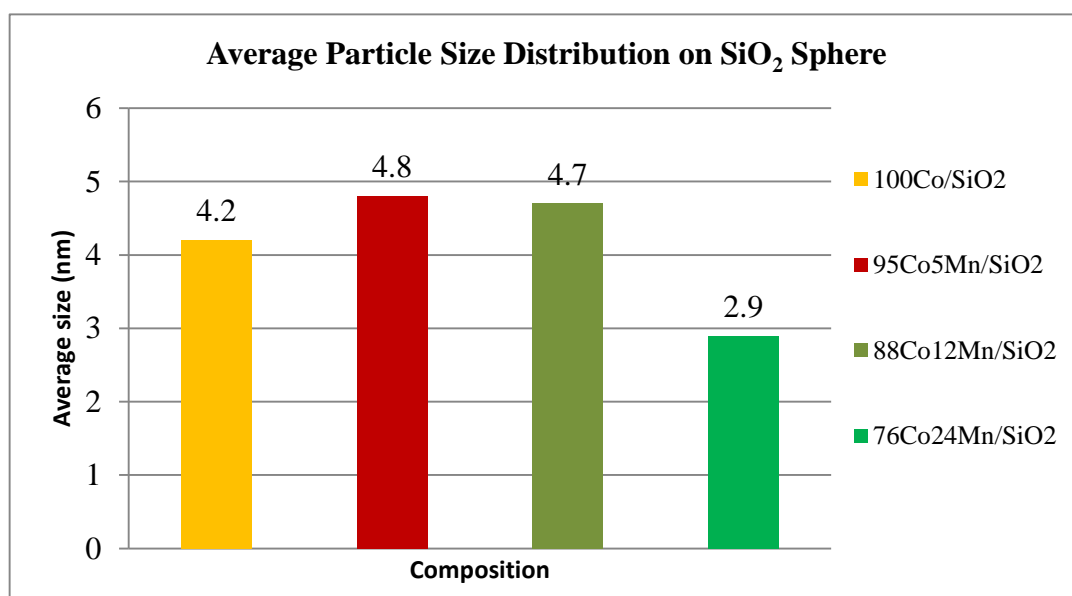


FIGURE 19. Average Particles Size Distribution on SiO<sub>2</sub> Sphere

FIGURE 15, 16, 17 and 18 shows the metal nanoparticles size distribution over SiO<sub>2</sub> support for the 100Co/SiO<sub>2</sub>, 95Co5Mn/SiO<sub>2</sub>, 88Co12Mn/SiO<sub>2</sub> and 76Co24Mn/SiO<sub>2</sub>. From the result, 76Co24Mn/SiO<sub>2</sub> has the smallest mean average metal size (M), 2.9 nm whereas 88Co12Mn/SiO<sub>2</sub> has the smallest population standard deviation (S), 1.7 nm. As being discussed, the narrowest particle size could lead to a better performance hence 88Co12Mn/SiO<sub>2</sub> catalyst has the most uniform metal distribution. While 76Co24Mn/SiO<sub>2</sub> has the smallest particle size, it has some big

metal attached on the SiO<sub>2</sub> surface which could decrease the reactivity of the surface site hence decreasing the performance of the nanocatalyst.

However, some of the particles are not distributed well in on the support surface because of the agglomeration of particles. The agglomeration might be due to some error on the methods during the synthesizing of the catalyst such as not continuous rate of stirring. Therefore the chemicals are not well-mixed and uniformly distributed. Other than that, the rate addition of THF will affect the dispersion of metal particles as well. A fast addition could lead to fast particle agglomeration and uncontrolled particle deposition on the silica support. Thus, the metal particles are agglomerate and not uniformly distributed on all SiO<sub>2</sub> sphere as shown in **FIGURE 20**.

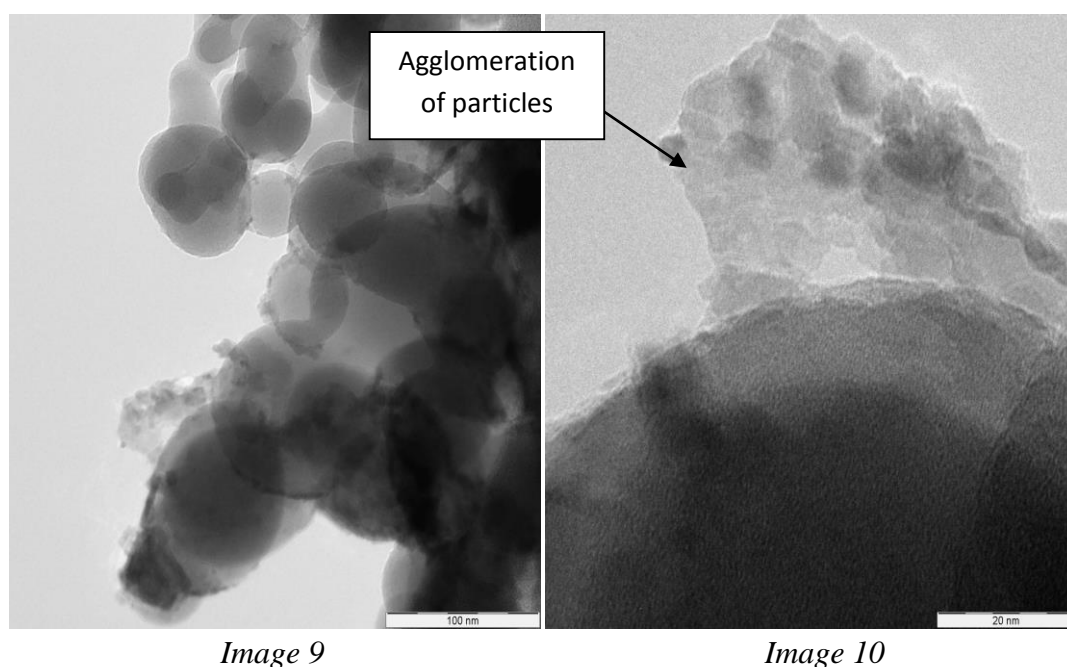
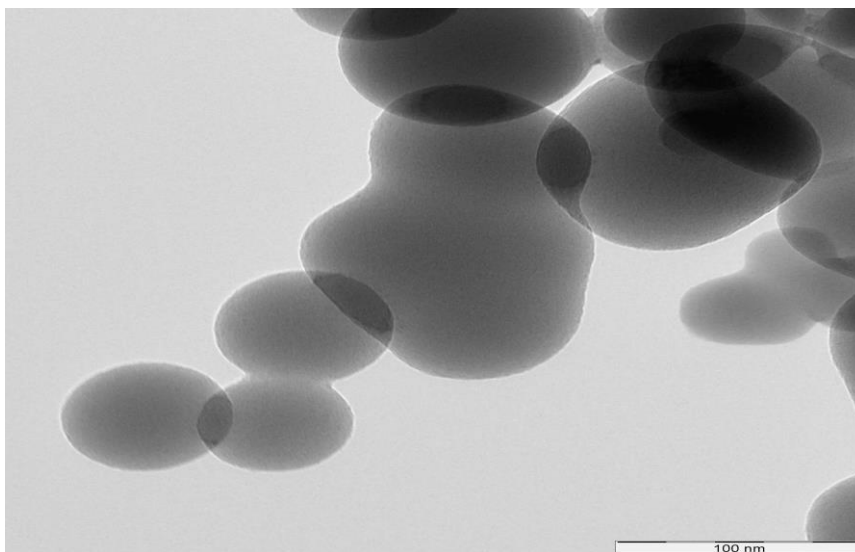


FIGURE 20. Agglomeration of Metal Nanoparticles in S1

In addition, there are also some areas of silica sphere which have no attached particles at all. This might cause by the SiO<sub>2</sub> sphere is not functionalized that makes the support is inert or the SiO<sub>2</sub> sphere was not dried enough thus the particles unable to attach to its surface. This condition indicates the dispersion problem on the

support surface and some recommendations are required. TEM image below shows the example of bare SiO<sub>2</sub> sphere area.



*Image 11*

FIGURE 21. Bare SiO<sub>2</sub> sphere in S2

#### **4.2.2 Field Emission Scanning Electron Microscopy (FESEM)**

The FESEM analysis provides a useful overview of the nanocatalyst. One of the advantages of FESEM is it can detect the name of metal nanoparticle which is attached on the SiO<sub>2</sub> sphere. In addition, it can indicate the size of the metal nanoparticle. One of the disadvantages of FESEM is the system cannot be used for higher resolution imaging to clearly display the distribution of metal particle on the SiO<sub>2</sub> sphere. The images obtained from FESEM are displayed in **APPENDIX 4**.

#### **4.2.3 Temperature Programmed Reduction (TPR)**

The reduction temperature can be predicted from the TPR graphs. **FIGURE 22** and shows the TPR graph for all nanocatalyst.

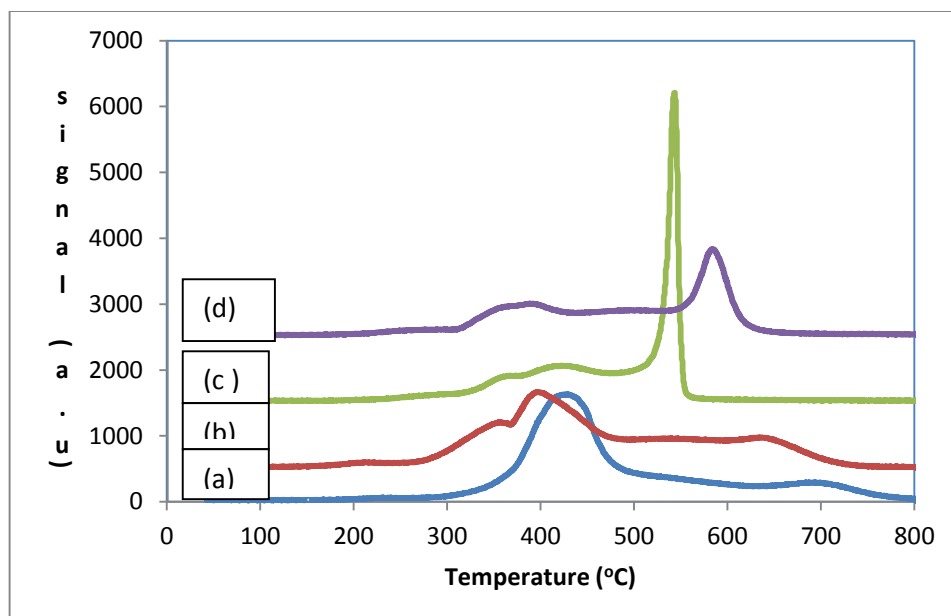


FIGURE 22. TPR profiles of (a) Co/SiO<sub>2</sub> (b) 95Co5Mn/SiO<sub>2</sub>. (c) 88Co12Mn/SiO<sub>2</sub> (d) 76Co24Mn/SiO<sub>2</sub>

The data from the graph are tabulated in **TABLE 6**.

TABLE 6. Reduction Temperature from TPR

| Sample | Composition               | Reduction Temperature (°C) |        |        |
|--------|---------------------------|----------------------------|--------|--------|
|        |                           | T1(°C)                     | T2(°C) | T3(°C) |
| S1     | 100Co/SiO <sub>2</sub>    | 419                        | 690    | -      |
| S2     | 95Co5Mn/SiO <sub>2</sub>  | 240                        | 370    | 645    |
| S3     | 88Co12Mn/SiO <sub>2</sub> | 350                        | 420    | 536    |
| S4     | 76Co24Mn/SiO <sub>2</sub> | 350                        | 380    | 600    |

FIGURE 22 shows the TPR profiles of the samples. For monometallic Co/SiO<sub>2</sub>, the reduction of Co<sub>3</sub>O<sub>4</sub> to CoO was observed at 419 °C and the high temperature peak (690 °C) was due to the reduction of CoO to Co. The presence of 5 wt% Mn shifted the second reduction peak to lower temperature (645 °C). Increasing the Mn content up to 12 wt% shifted the second reduction peak to an even lower temperature (536 °C), indicating enhancement in reducibility. The particle size of the 95Co5Mn/SiO<sub>2</sub> and 88Co12Mn/SiO<sub>2</sub> samples was found to be larger than that of Co/SiO<sub>2</sub>, which resulted in better reducibility. However, further increase in Mn content (24 wt%) was found to hamper the reduction of Co<sub>3</sub>O<sub>4</sub> possibly due to formation of Co-Mn spinels

and increase in metal-support interaction. The reduction temperature is lower as more Mn added to the Co until it's reached the optimum Mn addition (12 wt%). It was difficult to reduce nanocatalyst with the higher than 12 wt% percentage of Mn in the composition.

#### 4.2.4 Fischer-Tropsch Performance

Fischer-Tropsch performance was provided by the microreactor. **TABLE 7** shows the percentage of CO conversion and product distribution for each nanocatalyst.

TABLE 7. Reaction Result

| Experiment | Sample | Reduction Temperature (°C) | CO conversion (%) | HC product Selectivity (%) |                                |                 |
|------------|--------|----------------------------|-------------------|----------------------------|--------------------------------|-----------------|
|            |        |                            |                   | CH <sub>4</sub>            | C <sub>2</sub> -C <sub>4</sub> | C <sub>5+</sub> |
| 1          | S1     | 370                        | 2.7               | 28.3                       | 88.3                           | 3.4             |
| 2          | S2     | 370                        | 1.50              | 26.5                       | 69.3                           | 4.0             |
| 3          | S3     | 370                        | 1.34              | 24.2                       | 73.7                           | 2.1             |
| 4          | S4     | 370                        | 0.7               | 35.7                       | 63.4                           | 0.9             |
| 5          | S1     | 400                        | 10.85             | 18.6                       | 73.1                           | 8.3             |
| 6          | S2     | 400                        | 14.42             | 17.8                       | 72.4                           | 9.8             |
| 7          | S3     | 400                        | 20.5              | 15.2                       | 72.2                           | 12.6            |
| 8          | S4     | 400                        | 6.1               | 27.4                       | 69.7                           | 4.9             |

**TABLE 7** shows the lower CO conversion and product selectivity for 370 °C reduction temperature due to incomplete reduction process and the metal nanoparticles was not in its active form. CO conversion and product selectivity was getting higher when the reduction temperature for the reaction was increased to 400 °C. This shows that at 400 °C, the percentage of the metal nanoparticles reduced and convert to its active form was increased compared to the reduction temperature at 370 °C. Thus, the desired reduction temperature for the reaction is 400 °C since it produced the better result.

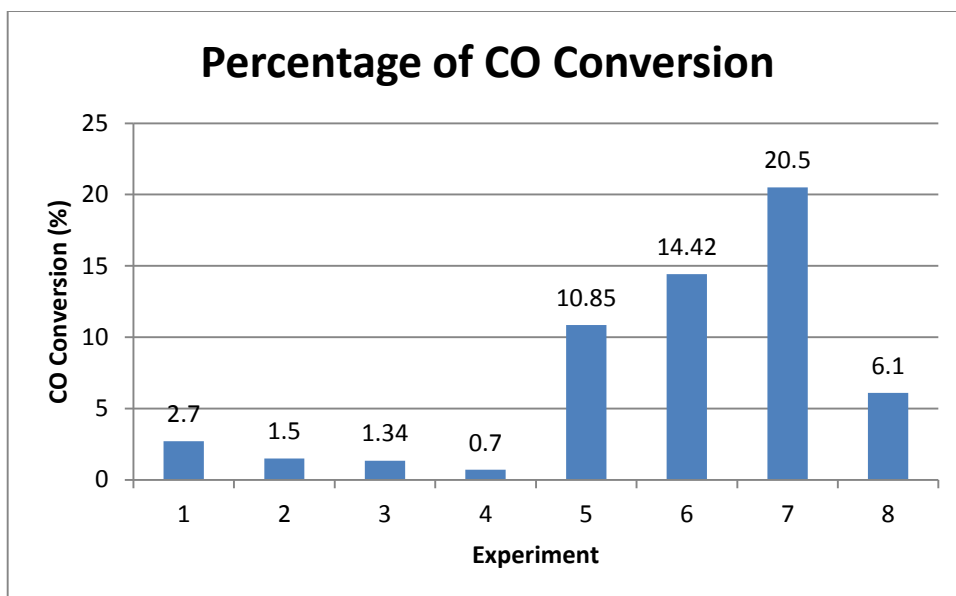


FIGURE 23. Percentage of CO Conversion at Different Composition

From **FIGURE 23**, for reduction temperature at 400 °C the highest CO conversion is 20.5% which is given by Experiment 7 (88Co12Mn/SiO<sub>2</sub>) while the lowest CO conversion is 6.1% which is given by Experiment 8 (76Co24Mn/SiO<sub>2</sub>). From the result, it can be hypothesized that increasing amount of Mn could increased the CO conversion but CO conversion was decreased if higher Mn percentage (24 wt%) was added to Co catalyst.

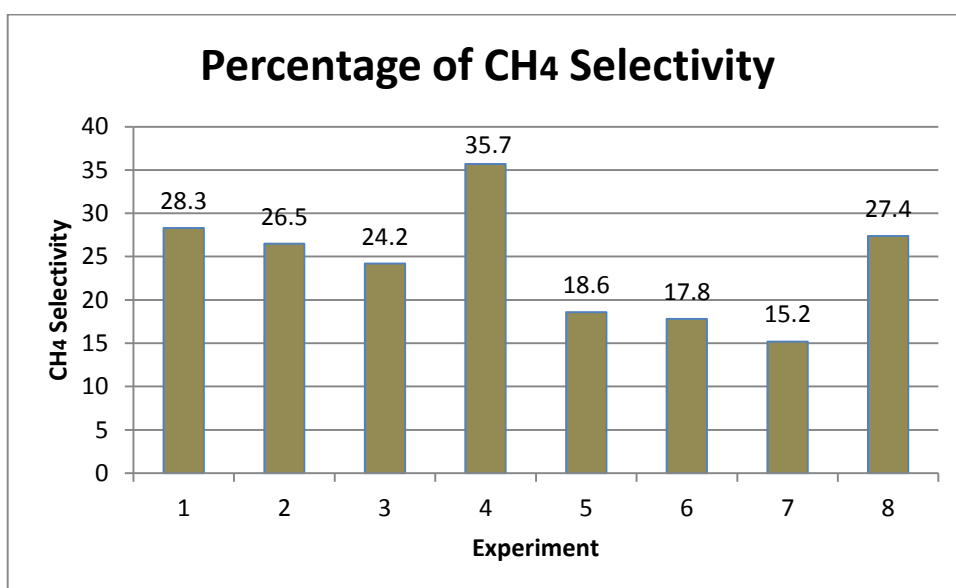


FIGURE 24. Percentage of CH<sub>4</sub> Selectivity at Different Composition



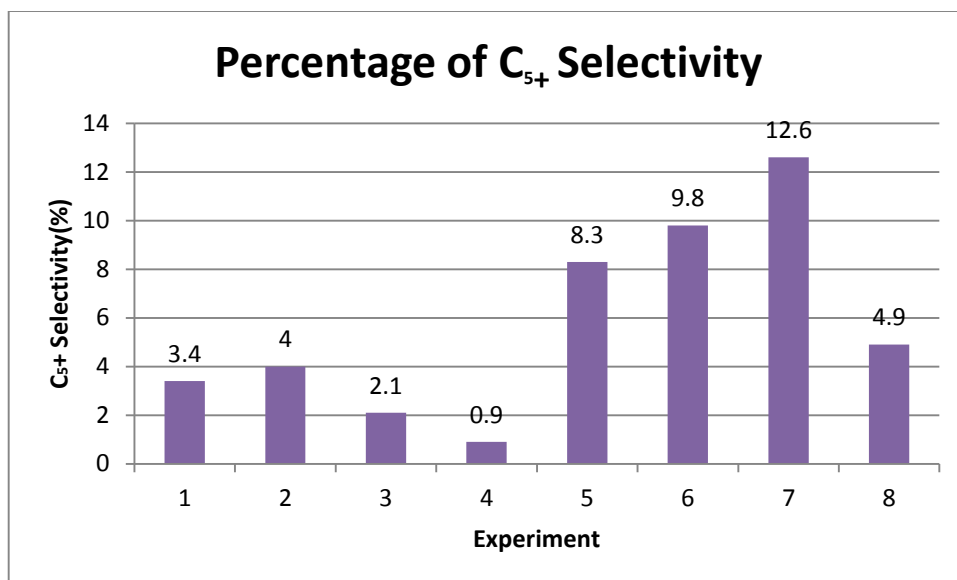


FIGURE 25. Percentage of C<sub>5+</sub> Selectivity at Different Composition

From **FIGURE 24** and **25**, the highest percentage of C<sub>5+</sub> selectivity is given by 88Co24Mn/SiO<sub>2</sub> which is 12.6% and the selectivity of C<sub>5+</sub> content is decreased to 4.9% as the amount of Mn increase to 24 wt%. In Fischer-Tropsch process, it is important to keep the catalyst at low methane selectivity and high selectivity for C<sub>5+</sub> product. From the bar chart, it can be concluded that 88Co12Mn/SiO<sub>2</sub> has the highest C<sub>5+</sub> selectivity and lower CH<sub>4</sub> production. The lower conversion of CO and C<sub>5+</sub> selectivity was might be due to the smaller nanoparticles size which can reduces the active site of the nanocatalyst. The other possibilities are sintering and poisoning of nanocatalyst has been occurred during the reaction as well as the presence of mixed compound that can reduce the catalytic activity and deactivate the nanocatalyst.

The result was compared with the other research work. According to Arne Dinse et al (2012), the CO conversion for unpromoted nanocatalyst which was synthesizes by incipient wetness impregnation method, 100Co/SiO<sub>2</sub> was 8.6% while C<sub>5+</sub> selectivity was 5.2%. Another comparison was made for the combination of cobalt and manganese. Arne Dinse reported that 88Co12Mn/SiO<sub>2</sub> has yield 5.6% CO conversion and 6.0% C<sub>5+</sub> selectivity. Those values is lower than what was achieved in the reaction of 100Co/SiO<sub>2</sub> and 88Co12Mn/SiO<sub>2</sub> for this project but the trend is the same for both of the works whereby CO conversion and C<sub>5+</sub> selectivity is highest when 12 wt% Mn was added to the Co. The other work which is using the precipitation method, Barbara Enst et al (1999) reported that 10% CO conversion

3.1% C<sub>5+</sub> selectivity was achieved in the FT reaction for 100Co/SiO<sub>2</sub>. The percentage of CO conversion and C<sub>5+</sub> selectivity is lower than what was achieved in this project for the same nanocatalyst formulation. For overall, the project has made an improvement on the reaction part to achieve the desired result.

The example of gas chromatograph (GC) spectra for sample 3 (88Co12Mn/SiO<sub>2</sub>) are shown in **APPENDIX 6**.

## CHAPTER 5

### CONCLUSION

In this project, the “Reverse Microemulsion Method” has been chosen to be experimented due to its exclusivity of preparation method and the advantages of the outcome nanocatalyst compared to other methods which are very typical in laboratory practices. Towards the production of better nanocatalyst performance, two type of metal namely Cobalt (Co) and Manganese (Mn) were mixed together to create an active bimetallic nanocatalyst which from various report, is proven to own more superior performance than the application of monometallic nanocatalyst, provided that the ratio between those two metals are divided wisely in the bimetallic nanocatalyst.

This project has been carried out using silica dioxides sphere ( $\text{SiO}_2$ ) as a support for Co/Mn nanocatalysts. The effects of different composition namely 100:0, 95:5, 88:12 and 76:24 have been experimented throughout the research. According to TEM result, average nanoparticles size found in all the nanocatalyst deposited on the  $\text{SiO}_2$  sphere were approximately in the range of 2-5 nm. The calculation made from TEM analysis imaging shows that 88Co12Mn/ $\text{SiO}_2$  nanocatalyst has the smallest population standard deviation which means it has the most uniform bimetallic nanoparticles distribution. Thus, bimetallic nanoparticles were dispersed better for the 88Co12Mn/ $\text{SiO}_2$  formulation compared to other composition. The average bimetallic nanoparticle size for 88Co12Mn/ $\text{SiO}_2$  was about 5 nm.

Based on Fischer-Tropsch performance of the microreactor, the highest CO conversion (20.5%) and  $\text{C}_{5+}$  selectivity (12.6%) was obtained over 88Co12Mn/ $\text{SiO}_2$  catalyst. However, increasing Mn content up to 24 wt% was found to be detrimental to the catalyst performance possibly due to formation of Co-Mn complex, changes in particle size distribution and metal-support interaction. From this result, it can be concluded that 88Co12Mn/ $\text{SiO}_2$  is the most suitable nanocatalyst for Fischer-

Tropsch process as it has the uniform distribution, larger average particle size, highest percentage of C<sub>5+</sub> selectivity and low production of methane. The smaller particle size of 76Co24Mn/SiO<sub>2</sub> make this nanocatalyst was not able to produces the better result for the reaction. Thus, further recommendation is required.

The result from TPR is quite significant when the relation was made between the reduction temperature from TPR and nanocatalyst catalytic activity performance, as it is hard to reduce the nanocatalyst with higher percentage of Mn (24 wt%). 76Co24Mn/SiO<sub>2</sub> was not capable to produce the higher conversion of CO and higher selectivity to desired product (C<sub>5+</sub>).

For recommendation, the focus is more to the preparation method which is the important part of the process. The unexpected result from this project might be caused by the any deviation from the reverse microemulsion steps for example the stirrer method. The overhead stirrer is recommended rather than current stirrer method, magnetic bar stirrer to stir the mixture. This is important to ensure the mixture is well-mixed and uniform rate of stirring that can lead to better dispersion of the metal nanoparticles and prevent the agglomeration of those nanoparticles. Next, the project needs to optimize the reduction temperature prior reaction to ensure metal active sites were present for the reaction. The current 400 °C reduction temperature was used for reduction process. The optimum reduction temperature needs to be determined through optimization process for safety and economic reason. The higher reduction temperature might be not suitable for the reaction because it is too dangerous and not economically feasible. Type of surfactant can affect the size, type of size distribution and structured of nanoparticles synthesized in reverse microemulsion. Therefore, the chosen of better surfactant than Triton X-114 can lead to the improvement on those factors. The project have met the objectives to synthesizes and characterizes the Co/Mn nanocatalyst supported on SiO<sub>2</sub> via reverse microemulsion and several analysis as well as to evaluate the performance of the nanocatalyst in Fischer-Tropsch reaction but more improvement are still required especially on the preparation steps and reaction optimization.

## REFERENCES

- Adesina, A. A. (1995). Hydrocarbon synthesis via fischer-tropsch reaction: travails and triumphs. *Applied Catalyst A:General*, 138, 345-367.
- Barbara, E. (1999). Preparation and characterization of Fischer-Tropsch active Co/SiO<sub>2</sub> catalysts. *Applied Catalyst A:General*, 186, 145-168.
- Chiesa, P., & Consonni, S. (2003). Second Annual Conference on Carbon Sequestration, Washington.
- Clean alternative fuels: Fischer-Tropsch. (2002) Retrieved from [www.afdc.energy.gov/pdfs/epa\\_fischer.pdf](http://www.afdc.energy.gov/pdfs/epa_fischer.pdf)
- Den Breejen, J.P., Frey, A.M., Yang, J., Holmen, A. et al. (2011). A highly active and selective manganese oxide promoted cobalt-on-silica Fischer-Tropsch catalyst. *Topics in Catalysis*, 54, 768-777.
- Dinse, A., Aigner, M., Markus, U., Gregory, R. J., & Alexis, T. B. (2012). Effect of Mn promotion on the activity and selectivity of Co/SiO<sub>2</sub> for fischer-tropsch synthesis. *Journal of Catalysis*, 288, 104-114.
- Duvenhage, D. J., & Coville, N. J. (1996). Fe:Co/TiO<sub>2</sub> bimetallic catalyst for the fischer-tropsch reaction 1. characterization and reactor studies. *Applied Catalyst A:General*, 153, 43-67.
- Herranz, T., Perez Alonso, F. J., Ojeda, M., & Terreros, P. (2006). Hydrogenation of carbon oxides over promoted Fe-Mn catalyst prepared by the microemulsion methodology. *Applied Catalyst A:General*, 311, 67.
- Herranz, T., Perez Alonso, F. J., Ojeda, M., & Terreros, P. (2006). Hydrogenation of carbon oxides over promoted Fe-Mn catalyst prepared by the microemulsion methodology. *Applied Catalyst A:General*, 311, 66.
- Lee, J.F., Chem, W.S., Lee, M.D., Dong, T.Y., Can, J. (1992). Fischer-Tropsch product distribution. *Chemical Engineering*, 70, 511..

Riedel, T., Claeys, M., Shulz, H., Schaub, G., Nam, S.S., Jun, K.W., Choi, M.J., Kishan, G., Lee, K.W. (1999). Comparative study of Fischer-Tropsch synthesis with H<sub>2</sub>/CO and H<sub>2</sub>/CO<sub>2</sub> syngas using Fe- and Co-based catalysts. *Applied Catalyst A: General*, 186, 201.

Steynberg, A. P. (2004). Chapter 1 introduction to Fischer-Tropsch technology. In André Steynberg and Mark Dry (Ed.), *Studies in surface science and catalysis* (pp. 1-63) Elsevier.

The early day of coal research (2006) Retrieved from [http://www.fe.doe.gov/aboutus/history/syntheticfuels\\_history.html](http://www.fe.doe.gov/aboutus/history/syntheticfuels_history.html)

Vannice, M.A. (1975). Catalyst for Fischer-Tropsch. *Catalyst*, 37, 228.

Zhang, Y., Liu, Y., Yang, G.H., Sun, S.L., Tsubaki, N. (2007). Effect of impregnation solvent on Co/SiO<sub>2</sub> catalyst for Fischer-Tropsch synthesis: A highly and stable catalyst with bimodal sized cobalt particles. *Applied Catalyst A: General*, 321, 79-85.

Zielinska-Jurek, A., Reszczyńska, J., Grabowska, E., & Zaleska, A. (2012). Nanoparticles preparation using microemulsion systems. In Dr. Reza Najjar (Ed), *Microemulsions-An Introduction to Properties and Applications* (pp. 229-232) InTech.

## APPENDIX

### APPENDIX 1.CALCULATION

#### Conversion from Mole Percentage (%) to Mass Percentage (%)

Convert the three selected different metal composition which are from previous research paper from mole percentage (%) to weight percentage (%) for comparison. The three different metal compositions are listed below which are not consist of pure cobalt and manganese.

1.  $Mn/Co = 0.05 \times 100 = 5 \text{ mole } \%$
2.  $Mn/Co = 0.125 \times 100 = 12.5 \text{ mole } \%$
3.  $Mn/Co = 0.25 = 25 \text{ mole } \%$

This is in mole percentage (%). Thus, convert to weight percentage (%) by assuming 100 moles total mixture.

#### 1. $Mn/Co=0.05$

For 100 moles total mixture, this composition has 5 mole Mn and 95 mole Co

$$\text{Weight of Mn} = 5 \text{ mol} \times \frac{54.9 \text{ g}}{\text{mol}} = 274.5 \text{ g Mn}$$

$$\text{Weight of Co} = 95 \text{ mol} \times \frac{58.9 \text{ g}}{\text{mol}} = 5595.5 \text{ g Co}$$

$$\text{Total weight} = 274.5 \text{ g Mn} + 5595.5 \text{ g Co} = 5870 \text{ g}$$

Weight percentage (%)

$$Mn = \frac{274.5 \text{ g}}{5870 \text{ g}} \times 100 = 4.7 \text{ wt\% Mn}$$

$$Co = \frac{5595.5 \text{ g}}{5870 \text{ g}} \times 100 = 95.3 \text{ wt\% Co}$$

## 2. Mn/Co = 0.125

For 100 moles total mixture, this composition has 12.5 mole Mn and 87.5 mole Co

$$\text{Weight of Mn} = 12.5 \text{ mol} \times \frac{54.9 \text{ g}}{\text{mol}} = 686.3 \text{ g Mn}$$

$$\text{Weight of Co} = 87.5 \text{ mol} \times \frac{58.9 \text{ g}}{\text{mol}} = 5153.8 \text{ g Co}$$

$$\text{Total weight} = 686.3 \text{ g Mn} + 5153.8 \text{ g Co} = 5840.1 \text{ g}$$

Weight percentage (%)

$$\text{Mn} = \frac{686.3 \text{ g}}{5840.1 \text{ g}} \times 100 = 11.8 \text{ wt\% Mn}$$

$$\text{Co} = \frac{5153.8 \text{ g}}{5840.1 \text{ g}} \times 100 = 88.2 \text{ wt\% Co}$$

## 3. Mn/Co = 0.25

For 100 moles total mixture, this composition has 25 mole Mn and 75 mole Co

$$\text{Weight of Mn} = 25 \text{ mol} \times \frac{54.9 \text{ g}}{\text{mol}} = 1372.5 \text{ g Mn}$$

$$\text{Weight of Co} = 75 \text{ mol} \times \frac{58.9 \text{ g}}{\text{mol}} = 4417.5 \text{ g Co}$$

$$\text{Total weight} = 1372.5 \text{ g Mn} + 4417.5 \text{ g Co} = 5790 \text{ g}$$

Weight percentage (%)

$$\text{Mn} = \frac{1372.5 \text{ g}}{5790 \text{ g}} \times 100 = 23.7 \text{ wt\% Mn}$$

$$\text{Co} = \frac{4417.5 \text{ g}}{5790 \text{ g}} \times 100 = 76.3 \text{ wt\% Co}$$

Therefore, the compositions in weight percentage (%) including the pure metal are tabulated below. Then, proceed with reactivity comparison between all different metal compositions.

TABLE 8. Metal Composition

| No of Sample | Composition of Co/Mn (10 wt %) |
|--------------|--------------------------------|
| 1            | 100:0                          |
| 2            | 95.3:4.7                       |
| 3            | 88.2:11.8                      |



|   |           |
|---|-----------|
| 4 | 76.3:23.7 |
| 5 | 0:100     |

Then, the calculation proceeds to calculate the mass needed for each composition with sample size 0.5 gram.

Sample size: 0.5 gram catalyst

Mass of catalyst = mass of metal + mass of support

Percentage (%) of metal loading: 10 wt% metal from the catalyst

Mass of support = Mass of Catalyst + Mass of metal

$$= 0.5 \text{ g} - (10/100 \times 0.5 \text{ g catalyst})$$

$$= 0.5 \text{ g} - 0.05 \text{ g metal}$$

$$= 0.45 \text{ g of support}$$

### Amount of Cobalt and Manganese Nitrate for catalyst preparation

As being discussed in **Chapter 3.2**, the weight percent of metal to be introduced inside the supporter is 10 wt% whereas the mass loading for silica for each sample is 0.45g. Thus, the appropriate amount of the metals is shown in the following table.

The calculation for each sample is displayed as below:

Information:

- Mass loading of silica : 0.45 g
- Molecular weight of 10 wt% Cobalt Nitrate  $\text{Co}(\text{NO}_3)_2 \cdot 6\text{H}_2\text{O}$  : 291.04 g/mol
- Molecular weight of 10 wt% Cobalt Nitrate  $\text{Mn}(\text{NO}_3)_2 \cdot 6\text{H}_2\text{O}$  : 287 g/mol

#### A) Co:Mn ; 100:0

For (Co:Mn at 100:0), 100% of metal loading is cobalt only, thus the mass of metal is 0.05 Cobalt which come in the form of  $\text{Co}(\text{NO}_3)_2 \cdot 6\text{H}_2\text{O}$ .

MW of Co = 59 g/mol

$$\frac{0.05 \text{ g Co}}{59 \frac{\text{g}}{\text{mol Co}}} \times 291.04 \text{ g/mol Co}(\text{NO}_3)_2 \cdot 6\text{H}_2\text{O} = 0.25 \text{ g Co}(\text{NO}_3)_2 \cdot 6\text{H}_2\text{O}$$

Therefore, in 0.25 g  $\text{Co}(\text{NO}_3)_2 \cdot 6\text{H}_2\text{O}$  there is 0.05g Co which is 10% from catalyst.

Hence, the amount of  $\text{Co}(\text{NO}_3)_2 \cdot 6\text{H}_2\text{O}$  needed = 0.25 g

**B) Co:Mn ; 95.3:4.7** , mass metal is constant for any ratio.

$$\begin{aligned} \text{Mass of metal} = 0.05 \text{ g of metal (10 wt\%)} &= \left[ \frac{5}{100} \times \frac{95.3}{100} \right] + \left[ \frac{5}{100} \times \frac{4.7}{100} \right] \\ &= 0.048 \text{ gCo} + 0.002 \text{ gMn} \end{aligned}$$

For Cobalt,

$$\frac{0.048 \text{ gCo}}{59 \text{ g/molCo}} \times 291.04 \text{ g/molCo}(\text{NO}_3)_2 \cdot 6\text{H}_2\text{O} = 0.24 \text{ gCo}(\text{NO}_3)_2 \cdot 6\text{H}_2\text{O}$$

For Manganese,

MW of Mn = 55 g/mol

$$\frac{0.002 \text{ gMn}}{55 \text{ g/molCo}} \times 287 \text{ g/molMn}(\text{NO}_3)_2 \cdot 6\text{H}_2\text{O} = 0.010 \text{ gMn}(\text{NO}_3)_2 \cdot 6\text{H}_2\text{O}$$

Hence, the amount of  $\text{Co}(\text{NO}_3)_2 \cdot 6\text{H}_2\text{O}$  needed = 0.24 g

Amount of  $\text{Mn}(\text{NO}_3)_2 \cdot 6\text{H}_2\text{O}$  needed = 0.0104 g

Total mass metal precursor = 0.24 g + 0.0104 g = 0.25 g

**C) Co:Mn ; 88.2:11.8**

$$\begin{aligned} \text{Mass of metal} = 0.05 \text{ g of metal (10 wt\%)} &= \left[ \frac{5}{100} \times \frac{88.2}{100} \right] + \left[ \frac{5}{100} \times \frac{11.8}{100} \right] \\ &= 0.044 \text{ gCo} + 0.006 \text{ gMn} \end{aligned}$$

For Cobalt,

$$\frac{0.044 \text{ gCo}}{59 \text{ g/molCo}} \times 291.04 \text{ g/molCo}(\text{NO}_3)_2 \cdot 6\text{H}_2\text{O} = 0.22 \text{ gCo}(\text{NO}_3)_2 \cdot 6\text{H}_2\text{O}$$

For Manganese,

$$\frac{0.006 \text{ gMn}}{55 \text{ g/molCo}} \times 287 \text{ g/molMn}(\text{NO}_3)_2 \cdot 6\text{H}_2\text{O} = 0.031 \text{ gMn}(\text{NO}_3)_2 \cdot 6\text{H}_2\text{O}$$

Hence, the amount of  $\text{Co}(\text{NO}_3)_2 \cdot 6\text{H}_2\text{O}$  needed = 0.22 g

Amount of  $\text{Mn}(\text{NO}_3)_2 \cdot 6\text{H}_2\text{O}$  needed = 0.031 g

Total mass metal precursor = 0.22 g + 0.031 g = 0.251 g

**D) Co:Mn ; 76.3:23.7**

$$\begin{aligned} \text{Mass of metal} &= 0.05 \text{ g of metal (10 wt\%)} = \left[ \frac{5}{100} \times \frac{76.3}{100} \right] + \left[ \frac{5}{100} \times \frac{23.7}{100} \right] \\ &= 0.038 \text{ g Co} + 0.012 \text{ g Mn} \end{aligned}$$

For Cobalt,

$$\frac{0.038 \text{ g Co}}{59 \text{ g/mol Co}} \times 291.04 \text{ g/mol Co(NO}_3)_2 \cdot 6\text{H}_2\text{O} = 0.19 \text{ g Co(NO}_3)_2 \cdot 6\text{H}_2\text{O}$$

For Manganese,

$$\frac{0.012 \text{ g Mn}}{55 \text{ g/mol Co}} \times 287 \text{ g/mol Mn(NO}_3)_2 \cdot 6\text{H}_2\text{O} = 0.063 \text{ g Mn(NO}_3)_2 \cdot 6\text{H}_2\text{O}$$

Hence, the amount of  $\text{Co(NO}_3)_2 \cdot 6\text{H}_2\text{O}$  needed = 0.19 g

Amount of  $\text{Mn(NO}_3)_2 \cdot 6\text{H}_2\text{O}$  needed = 0.063 g

Total mass metal precursor = 0.19 g + 0.063 g = 0.253 g

**E) Co:Mn ; 0:100**

$$\frac{0.05 \text{ g Co}}{55 \frac{\text{g}}{\text{mol Co}}} \times 287 \text{ g/mol Mn(NO}_3)_2 \cdot 6\text{H}_2\text{O} = 0.26 \text{ g Mn(NO}_3)_2 \cdot 6\text{H}_2\text{O}$$

Therefore, in 0.26 g  $\text{Mn(NO}_3)_2 \cdot 6\text{H}_2\text{O}$  there is 0.05g Mn which is 10% from catalyst.

Hence, the amount of  $\text{Co(NO}_3)_2 \cdot 6\text{H}_2\text{O}$  needed = 0.26 g

Table 9. Appropriate Amount of Metal

| Samples                         |                      |                         |                          |                          |                      |
|---------------------------------|----------------------|-------------------------|--------------------------|--------------------------|----------------------|
| No.                             | A                    | B                       | C                        | D                        | E                    |
| <b>Composition</b>              | Co : Mn<br>(100 : 0) | Co : Mn<br>(95.3 : 4.7) | Co : Mn<br>(88.2 : 11.8) | Co : Mn<br>(76.3 : 23.7) | Co : Mn<br>(0 : 100) |
| <b>Amount of Co Nitrate (g)</b> | 0.25                 | 0.24                    | 0.22                     | 0.19                     | 0.26                 |
| <b>Amount of Mn Nitrate (g)</b> | -                    | 0.0104                  | 0.031                    | 0.063                    | -                    |
| <b>Net Total (g)</b>            | 0.25                 | 0.25                    | 0.251                    | 0.253                    | 0.26                 |

### Amount of water to surfactant

Base on previous research work, the suitable molarity of Triton X-114 in the cyclohexane is 0.2 molar and the optimum molar ratio of water to surfactant is 3:1.

$$\text{Molarity Triton X-114} = 0.2 \text{ M}$$

$$\text{Mol of Triton} = \text{Molarity (M)} \times \text{Volume (L)}$$

$$= 0.2 \text{ M} \times 0.1 \text{ L}$$

$$= 0.02 \text{ mol}$$

As from the experiment, the ratio of 3:1 (water-to-surfactant) is best suited with 0.02 molarity of Triton X-114 in cyclohexane which forms a homogenous solution at its critical micelle concentration. The calculation to determine the mass of Triton X-114 and water needed are as follows:

H<sub>2</sub>O : Triton X-114

$$3 : 1$$

$$0.06 : 0.02$$

$$\text{Mass of Triton X-114} = 0.02 \text{ mol} \times 558.75 \text{ g/mol Triton X-114}$$

$$= 11.175 \text{ g Triton X-114}$$

$$n_{H_2O} = \frac{n_{H_2O}}{MW_{H_2O}}$$

$$\text{Mass H}_2\text{O} = n_{H_2O} \times MW_{H_2O}$$

$$= 0.06 \text{ mol} \times 18 \text{ g/mol}$$

$$= 1.08 \text{ g H}_2\text{O}$$

### A) Co:Mn ; 100: 0

$$291.04 \text{ g Co(NO}_3)_2 \cdot 6\text{H}_2\text{O} \rightarrow 6 (18) \text{ g H}_2\text{O} = 108 \text{ g H}_2\text{O}$$

$$\frac{108 \text{ g H}_2\text{O}}{291.04 \text{ g Co(NO}_3)_2 \cdot 6\text{H}_2\text{O}} = 0.37 \text{ g H}_2\text{O in 1 g Co(NO}_3)_2 \cdot 6\text{H}_2\text{O}$$

Therefore for 0.25 g Co(NO<sub>3</sub>)<sub>2</sub>·6H<sub>2</sub>O → 0.09 g H<sub>2</sub>O (*Mass of water already in metal precursor*)

$$\text{Mass of H}_2\text{O required} = \text{Mass H}_2\text{O} - \text{Mass H}_2\text{O for 0.25 g Co(NO}_3)_2 \cdot 6\text{H}_2\text{O}$$

$$= 1.08 \text{ g} - 0.09 \text{ g}$$

$$= 0.99 \text{ g H}_2\text{O}$$

**B) Co:Mn ; 95:5**

$$287 \text{ g Mn(NO}_3)_2 \cdot 6\text{H}_2\text{O} \rightarrow 6 (18) \text{ g H}_2\text{O} = 108 \text{ g H}_2\text{O}$$

$$\frac{108 \text{ g H}_2\text{O}}{287 \text{ g Mn(NO}_3)_2 \cdot 6\text{H}_2\text{O}} = 0.38 \text{ g H}_2\text{O in 1 g Mn(NO}_3)_2 \cdot 6\text{H}_2\text{O}$$

$$\text{Therefore for } 0.010 \text{ g Mn(NO}_3)_2 \cdot 6\text{H}_2\text{O} \rightarrow 0.004 \text{ g H}_2\text{O}$$

$$\text{and } 0.24 \text{ g Co(NO}_3)_2 \cdot 6\text{H}_2\text{O} \rightarrow 0.09 \text{ g H}_2\text{O}$$

$$\text{Mass of H}_2\text{O required} = 1.08 \text{ g} - 0.004 \text{ g} - 0.088 \text{ g}$$

$$= 0.988 \text{ g H}_2\text{O}$$

**C) Co:Mn ; 88:12**

$$0.031 \text{ g Mn(NO}_3)_2 \cdot 6\text{H}_2\text{O} \rightarrow 0.012 \text{ g H}_2\text{O}$$

$$0.22 \text{ g Co(NO}_3)_2 \cdot 6\text{H}_2\text{O} \rightarrow 0.081 \text{ g H}_2\text{O}$$

$$\text{Mass of H}_2\text{O required} = 1.08 \text{ g} - 0.012 \text{ g} - 0.081 \text{ g}$$

$$= 0.987 \text{ g H}_2\text{O}$$

**D) Co:Mn ; 76:24**

$$0.063 \text{ g Mn(NO}_3)_2 \cdot 6\text{H}_2\text{O} \rightarrow 0.024 \text{ g H}_2\text{O}$$

$$0.19 \text{ g Co(NO}_3)_2 \cdot 6\text{H}_2\text{O} \rightarrow 0.07 \text{ g H}_2\text{O}$$

$$\text{Mass of H}_2\text{O required} = 1.08 \text{ g} - 0.024 \text{ g} - 0.07 \text{ g}$$

$$= 0.986 \text{ g H}_2\text{O}$$

**E) Co:Mn ; 0:100**

$$0.26 \text{ g Mn(NO}_3)_2 \cdot 6\text{H}_2\text{O} \rightarrow 0.10 \text{ g H}_2\text{O}$$

$$\text{Mass of H}_2\text{O required} = 1.08 \text{ g} - 0.10$$

$$= 0.98 \text{ g H}_2\text{O}$$

TABLE 10.Amount of Water to Surfactant

| No.   | Samples |        |        |        |        |
|---|---------|--------|--------|--------|--------|
|   | A       | B      | C      | D      | E      |
| <b>Molar Ratio</b>                          | 3:1     | 3:1    | 3:1    | 3:1    | 3:1    |
| <b>Mass Triton X-114 (g)</b>                | 11.175  | 11.175 | 11.175 | 11.175 | 11.175 |
| <b>Mass of Water (g)</b>                    | 1.08    | 1.08   | 1.08   | 1.08   | 1.08   |
| <b>Mass of Water in Metal precursor (g)</b> | 0.09    | 0.092  | 0.093  | 0.094  | 0.10   |
| <b>Mass of Water Required (g)</b>           | 0.99    | 0.988  | 0.987  | 0.986  | 0.98   |

### Amount of Hydrazine

Another chemical which is added into each sample is Hydrazine (N<sub>2</sub>H<sub>2</sub>). Hydrazine is added into each sample solution to improve the metal nanoparticle formation in the core of water micelles by reducing cobalt oxide and manganese oxide. Hydrazine is inserted at a ratio of 10:1 (hydrazine- Co/Mn) in each sample and the calculations are as follows:

n Hydrazine : n Metal (total for both Co and Mn)

10 : 1 (molar ratio)

#### A) Co:Mn ; 100:0

Mass of Co = 0.05 g

$$n = \frac{MassCo}{MWCo} = \frac{0.05 \text{ g}}{59 \text{ g/mol}} = 0.0008 \text{ molCo}$$

Therefore the mol ratio for hydrazine to pure cobalt is 0.008:0.0008

$$\begin{aligned} \text{Mass of Hydrazine} &= 0.008 \text{ mol} \times 32.05 \text{ g/mol hydrazine} \\ &= 0.2564 \text{ g hydrazine} \end{aligned}$$

**B) Co:Mn ; 95:5**

Mass of Co = 0.048 g

$$n = \frac{MassCo}{MWCo} = \frac{0.048 \text{ g}}{59 \text{ g/mol}} = 0.0008 \text{ molCo}$$

Mass of Mn = 0.002 g

$$n = \frac{MassMn}{MWMn} = \frac{0.002 \text{ g}}{55 \text{ g/mol}} = 0.00004 \text{ molMn}$$

Total number of mol = 0.0008 + 0.00004 = 0.00084

Therefore the mol ratio for hydrazine to (Co:Mn ; 95.3:4.7) is 0.0084:0.00084

Mass of Hydrazine = 0.0084 mol x 32.05 g/mol hydrazine

$$= 0.2692 \text{ g hydrazine}$$

**C) Co:Mn ; 88:12**

Mass of Co = 0.044 g

$$n = \frac{MassCo}{MWCo} = \frac{0.044 \text{ g}}{59 \text{ g/mol}} = 0.0007 \text{ molCo}$$

Mass of Mn = 0.006 g

$$n = \frac{MassMn}{MWMn} = \frac{0.006 \text{ g}}{55 \text{ g/mol}} = 0.00011 \text{ molMn}$$

Total number of mol = 0.0007 + 0.00011 = 0.00081

Therefore the mol ratio for hydrazine to (Co:Mn ; 88.2:11.8) is 0.0081:0.00081

Mass of Hydrazine = 0.0081 mol x 32.05 g/mol hydrazine

$$= 0.2596 \text{ g hydrazine}$$

**D) Co:Mn ; 76:24**

Mass of Co = 0.038 g

$$n = \frac{MassCo}{MWCo} = \frac{0.038 \text{ g}}{59 \text{ g/mol}} = 0.0006 \text{ molCo}$$

Mass of Mn = 0.012 g

$$n = \frac{MassMn}{MWMn} = \frac{0.012 \text{ g}}{55 \text{ g/mol}} = 0.00022 \text{ molMn}$$

Total number of mol = 0.0006 + 0.00022 = 0.00082

Therefore the mol ratio for hydrazine to (Co:Mn ; 76.3:23.7) is 0.0082:0.00082

Mass of Hydrazine = 0.0082 mol x 32.05 g/mol hydrazine

$$= 0.2628 \text{ g hydrazine}$$

**E) Co:Mn ; 0:100**

Mass of Mn = 0.05 g

$$n = \frac{\text{MassMn}}{\text{MWMn}} = \frac{0.05 \text{ g}}{55 \text{ g/mol}} = 0.0009 \text{ molMn}$$

Therefore the mol ratio for hydrazine to pure manganese is 0.009:0.0009

Mass of Hydrazine = 0.009 mol x 32.05 g/mol hydrazine

$$= 0.2885 \text{ g hydrazine}$$

TABLE 11.Amount of Hydrazine vs. Co/Mn

| <b>Samples</b>           |        |         |         |         |        |
|--------------------------|--------|---------|---------|---------|--------|
| <b>No.</b>               | A      | B       | C       | D       | E      |
| <b>Total amount of</b>   | 0.25   | 0.25    | 0.251   | 0.253   | 0.26   |
| <b>Co and Mn Nitrate</b> |        |         |         |         |        |
| <b>Total mol of Co</b>   | 0.0008 | 0.00084 | 0.00081 | 0.00082 | 0.0009 |
| <b>and Fe Nitrate</b>    |        |         |         |         |        |
| <b>Molar Ratio</b>       | 10:1   | 10:1    | 10:1    | 10:1    | 10:1   |
| <b>Amount of</b>         | 0.2564 | 0.2692  | 0.2596  | 0.2628  | 0.2885 |
| <b>Hydrazine (g)</b>     |        |         |         |         |        |



APPENDIX 2.KEY MILESTONE

| Activities   | FYP 1 |   |   |   |   |   |   |   |   |    |    |    |    |    | FYP 2 |   |   |   |   |   |   |   |   |    |    |    |    |    |
|--|-------|---|---|---|---|---|---|---|---|----|----|----|----|----|-------|---|---|---|---|---|---|---|---|----|----|----|----|----|
|  | 1     | 2 | 3 | 4 | 5 | 6 | 7 | 8 | 9 | 10 | 11 | 12 | 13 | 14 | 1     | 2 | 3 | 4 | 5 | 6 | 7 | 8 | 9 | 10 | 11 | 12 | 13 | 14 |
| Identify the purpose of this research project  |       |   | █ |   |   |   |   |   |   |    |    |    |    |    |       |   |   |   |   |   |   |   |   |    |    |    |    |    |
| Critical literature review and identify the chemical needed  |       |   |   |   |   |   |   |   |   | █  |    |    |    |    |       |   |   |   |   |   |   |   |   |    |    |    |    |    |
| Design the experimental procedures to synthesize Co/Mn nanocatalyst using reverse microemulsion method |       |   |   |   |   |   |   |   |   |    |    |    | █  |    |       |   |   |   |   |   |   |   |   |    |    |    |    |    |
| Study the analysis procedures for characterization of catalyst   |       |   |   |   |   |   |   |   |   |    |    |    |    |    |       |   |   |   |   |   | █ |   |   |    |    |    |    |    |
| Study the activity of catalyst on Fischer-Tropsch reaction   |       |   |   |   |   |   |   |   |   |    |    |    |    |    |       |   |   |   |   |   |   |   | █ |    |    |    |    |    |
| Data analysis and interpretation   |       |   |   |   |   |   |   |   |   |    |    |    |    |    |       |   |   |   |   |   |   |   |   |    |    | █  |    |    |
| Proper documentation of findings   |       |   |   |   |   |   |   |   |   |    |    |    |    |    |       |   |   |   |   |   |   |   |   |    |    |    | █  |    |

### APPENDIX 3.GANTT CHART

| Activities   | FYP 1 |   |   |   |   |   |   |   |   |    |    |    |    |    | FYP 2 |   |   |   |   |   |   |   |   |    |    |    |    |    |
|--|-------|---|---|---|---|---|---|---|---|----|----|----|----|----|-------|---|---|---|---|---|---|---|---|----|----|----|----|----|
|  | 1     | 2 | 3 | 4 | 5 | 6 | 7 | 8 | 9 | 10 | 11 | 12 | 13 | 14 | 1     | 2 | 3 | 4 | 5 | 6 | 7 | 8 | 9 | 10 | 11 | 12 | 13 | 14 |
| Critical literature review on Fischer-Tropsch reaction, bimetallic nanocatalyst, and reverse microemulsion method. | █     | █ | █ | █ | █ |   |   |   |   |    |    |    |    |    |       |   |   |   |   |   |   |   |   |    |    |    |    |    |
| Requisition of chemicals & laboratory apparatus  |       |   |   |   |   | █ | █ | █ | █ | █  |    |    |    |    |       |   |   |   |   |   |   |   |   |    |    |    |    |    |
| Synthesis of Co/Mn nanocatalyst using reverse microemulsion method   |       |   |   |   |   |   |   |   |   |    | █  | █  | █  | █  | █     | █ | █ |   |   |   |   |   |   |    |    |    |    |    |
| Characterization of Co/Mn nanocatalyst.  |       |   |   |   |   |   |   |   |   |    |    |    |    |    | █     | █ | █ | █ | █ |   |   |   |   |    |    |    |    |    |
| Study the activity of catalyst on Fischer-Tropsch reaction.  |       |   |   |   |   |   |   |   |   |    |    |    |    |    |       |   |   |   |   | █ | █ | █ | █ |    |    |    |    |    |
| Data analysis and interpretation.  |       |   |   |   |   |   |   |   |   |    |    |    |    |    |       |   |   |   |   |   |   |   |   | █  | █  | █  | █  |    |

## APPENDIX 4.FESEM

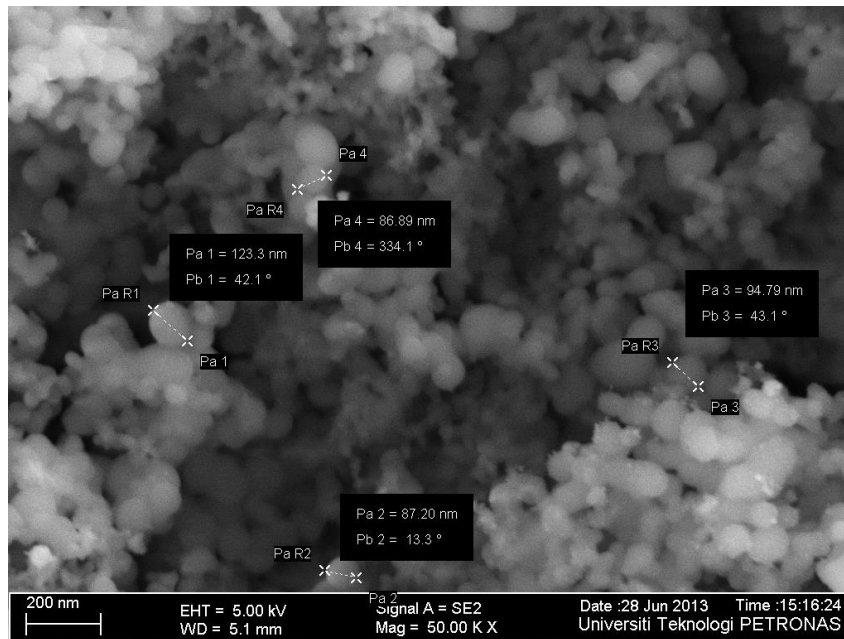


FIGURE 26.FESEM image on 100Co/SiO<sub>2</sub>

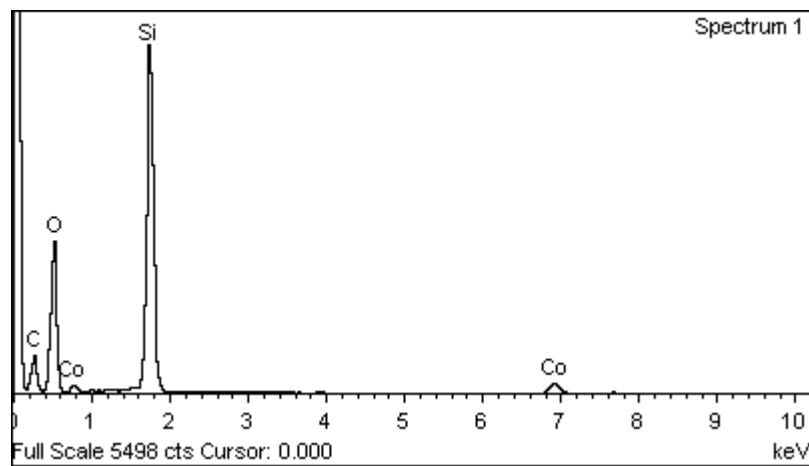


FIGURE 27.Spectrum Processing on 100Co/SiO<sub>2</sub>

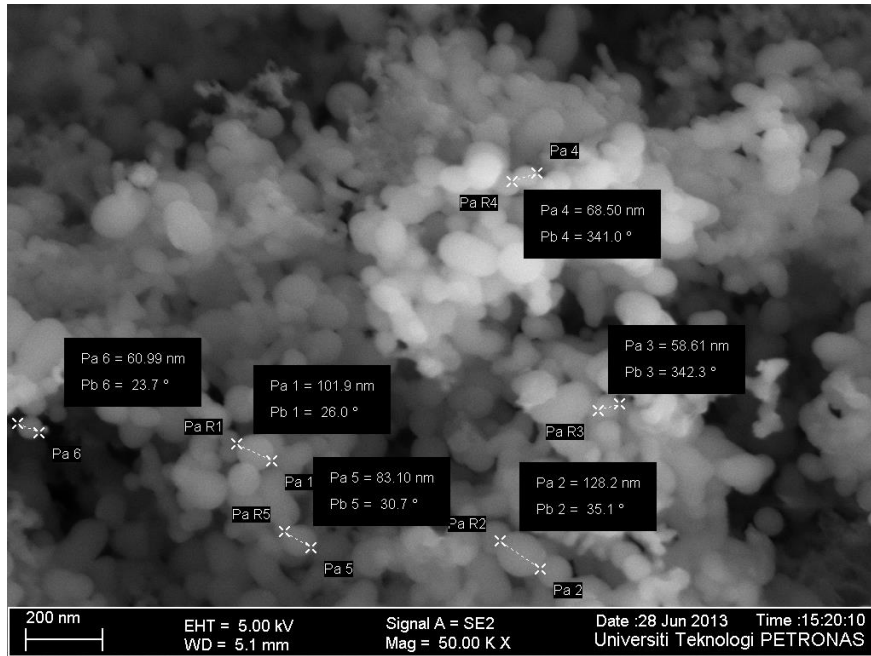


FIGURE 28.FESEM image on 95Co5Mn/SiO<sub>2</sub>

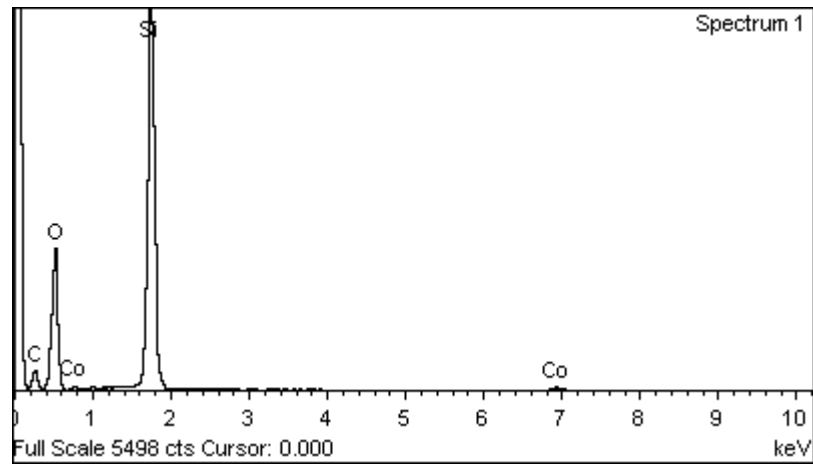
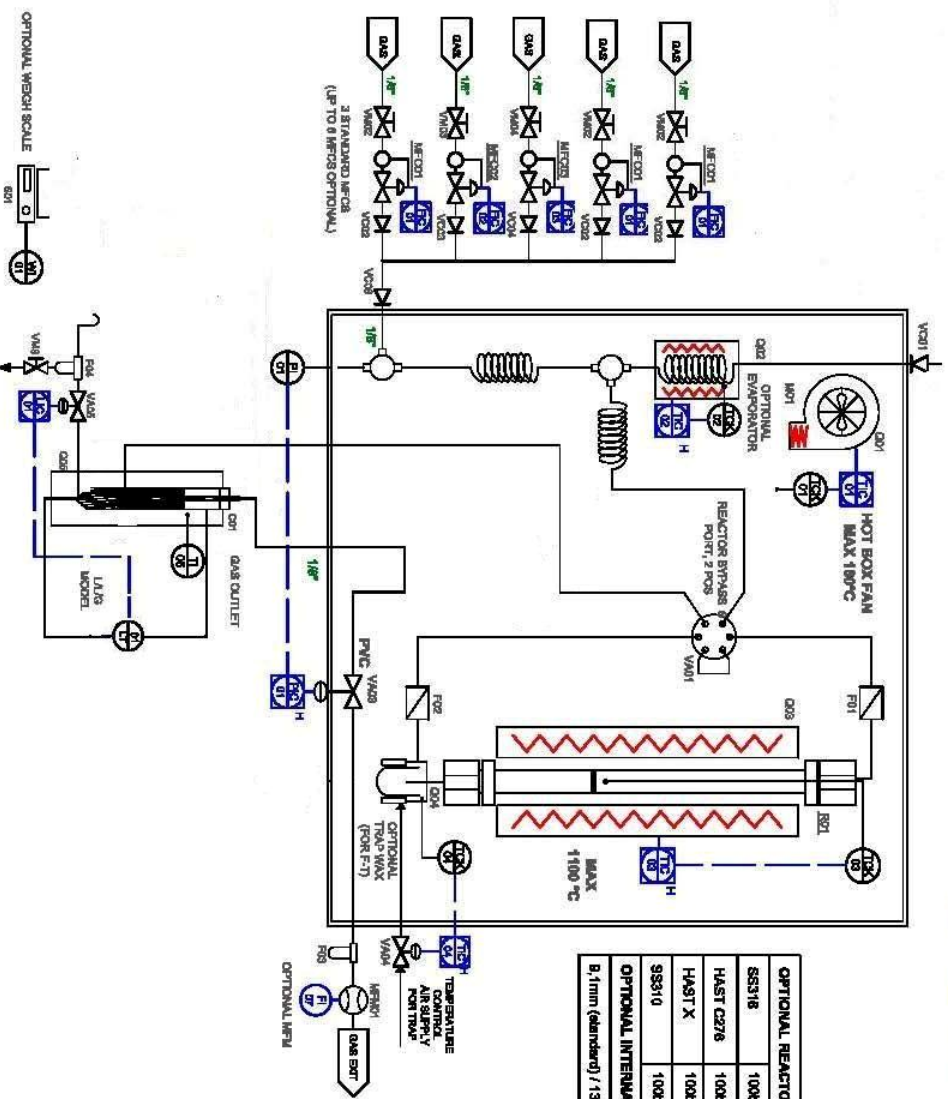


FIGURE 29.Spectrum Processing on 95Co5Mn/SiO<sub>2</sub>

APPENDIX 5.  
SCHEMATIC DRAWING- MICROACTIVITY REFERENCES REACTOR

APPENDIX 6.

GAS CHROMATOGRAPH (GC) SPECTRA FOR SAMPLE 3 ( $^{88}\text{Co}^{12}\text{Mn}/\text{SiO}_2$ )



|  |                |             |  |
|--|----------------|-------------|--|
| <b>OPTIONAL REACTOR MOC :</b>              |                |             |  |
| SS316                                      | 100bar @ 850°C | Max. 700°C  |  |
| HAST C276                                  | 100bar @ 850°C | Max. 1050°C |  |
| HAST X                                     | 100bar @ 800°C | Max. 1150°C |  |
| S3310                                      | 100bar @ 850°C | Max. 1100°C |  |
| <b>OPTIONAL INTERNAL DIAMETERS :</b>       |                |             |  |
| B: 1mm (standard) / 13,1mm / 17,5mm / 23mm |                |             |  |

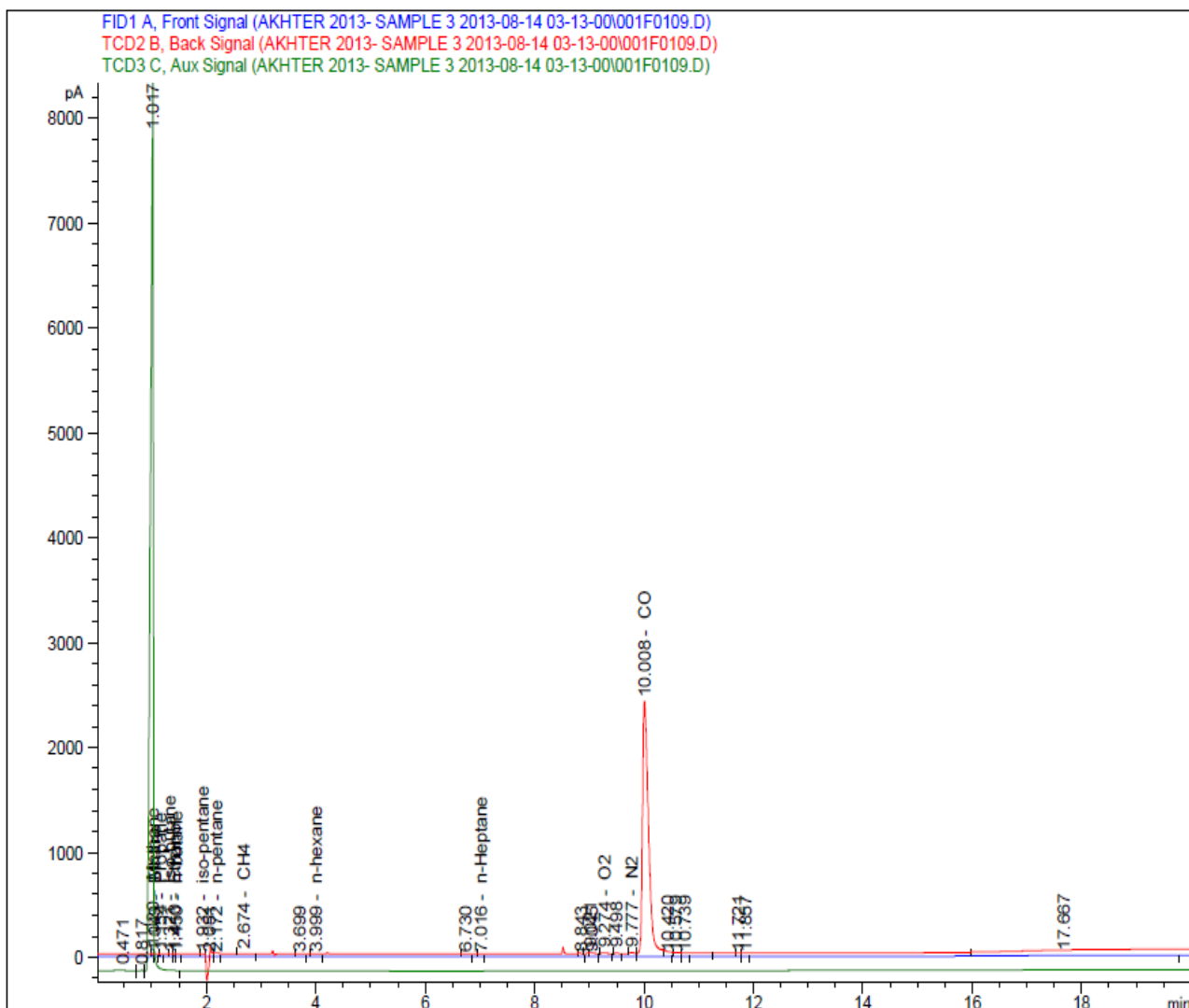
|                                     |                                    |
|-------------------------------------|------------------------------------|
| <input checked="" type="checkbox"/> | MANUAL OPERATED VALVES             |
| <input checked="" type="checkbox"/> | MANUAL OPERATED BALL VALVE         |
| <input checked="" type="checkbox"/> | CHECK VALVE                        |
| <input checked="" type="checkbox"/> | BACK PRESSURE VALVE                |
| <input checked="" type="checkbox"/> | ACTUATED VALVES                    |
| <input checked="" type="checkbox"/> | V01 & PORTZPORTION VALVE           |
| <input checked="" type="checkbox"/> | MICROMETRIC SERVO-CONTROLLED VALVE |
| <b>INSTRUMENTS</b>                  |                                    |
| <input checked="" type="checkbox"/> | IN-LINE FILTER                     |
| <input checked="" type="checkbox"/> | MASS FLOW CONTROLLER               |
| <input checked="" type="checkbox"/> | INSTRUMENTATION & CONTROL          |
| <input checked="" type="checkbox"/> | THERMOCOUPLE K-TYPE                |
| <input checked="" type="checkbox"/> | TEMPERATURE CONTROL                |
| <input checked="" type="checkbox"/> | PRESSURE CONTROL                   |
| <input checked="" type="checkbox"/> | LEVEL SENSOR                       |
| <input checked="" type="checkbox"/> | LEVEL CONTROL                      |

|   |     |      |            |             |                |         |            |             |         |      |            |             |     |
|---|-----|------|------------|-------------|----------------|---------|------------|-------------|---------|------|------------|-------------|-----|
| Rev   | 0   | DATE | 11/11/2023 | DESCRIPTION | Initial        | DATE    | 11/11/2023 | DESCRIPTION | Checked | DATE | 11/11/2023 | DESCRIPTION |     |
| REV   | 0   | DATE | 11/11/2023 | DESCRIPTION | Dibujó Inicial | DWN     | CHKD       | APPD        | APPD    | APPD | APPD       | APPD        |     |
| <p>THIS DRAWING IS CONFIDENTIAL. THE PARTIAL OR TOTAL REPRODUCTION OF IT IS FORBIDDEN WITHOUT A WRITTEN AUTHORIZATION FROM RESPONSIBLE.</p> |     |      |            |             |                |         |            |             |         |      |            |             |     |
| SCALE   | 1/1 | DATE | 11/11/2023 | DRAWN BY    | AM             | CHKD BY | AM         | APPD BY     | AM      | SIZE | A4         | DRAWING NO. | REV |
| SCALE   | 1/1 | DATE | 11/11/2023 | DRAWN BY    | AM             | CHKD BY | AM         | APPD BY     | AM      | SIZE | A4         | DRAWING NO. | REV |
| <p>ORGANIZATION: PID EngTech</p>  |     |      |            |             |                |         |            |             |         |      |            |             |     |

Data File C:\CHEM32\1\DATA\AKHTER 2013- SAMPLE 3 2013-08-14 03-13-00\001F0109.D  
Sample Name: L10

```
=====
Acq. Operator   : Ali                               Seq. Line :    1
Acq. Instrument : Instrument 1                       Location  : Vial 1
Injection Date  : 8/14/2013 6:42:27 AM              Inj       :    9
                                                    Inj Volume: 1000 µl

Acq. Method     : C:\CHEM32\1\DATA\AKHTER 2013- SAMPLE 3 2013-08-14 03-13-00\FULL.M
Last changed    : 2/22/2012 1:30:32 PM by Ali
Analysis Method : C:\CHEM32\1\METHODS\FULL.M
Last changed    : 2/22/2012 1:30:32 PM by Ali
Method Info     : RGA and NGA
=====
```



External Standard Report

```
=====
Sorted By      :      Signal
Calib. Data Modified :      6/14/2011 10:50:21 PM
Multiplier:    :      1.0000
Dilution:     :      1.0000
Use Multiplier & Dilution Factor with ISTDs
=====
```